Magmatic Processes During the Prolonged Pu'u 'O'o Eruption of Kilauea Volcano, Hawaii

MICHAEL O. GARCIA[1]*, AARON J. PIETRUSZKA[1]†, J. M. RHODES[2] AND KIERSTIN SWANSON[1]

[1]HAWAII CENTER FOR VOLCANOLOGY, DEPARTMENT OF GEOLOGY AND GEOPHYSICS, UNIVERSITY OF HAWAII, HONOLULU, HI 96822, USA

[2]DEPARTMENT OF GEOSCIENCES, UNIVERSITY OF MASSACHUSETTS, AMHERST, MA 01003, USA

The Pu'u 'O'o eruption is exceptional among historical eruptions of Kilauea Volcano for its long duration ($\sim$ 17 years and continuing), large volume ($\sim$ 2 km^3), wide compositional range (5·6–10·1 wt % MgO) and the detailed monitoring of its activity. The prolonged period of vigorous effusion ($\sim$ 300 000 m^3/day) and the simple phenocryst mineralogy of the lavas (essentially only olivine) has allowed us to examine the volcano's crustal and mantle magmatic processes. Here we present new petrologic data for lavas erupted from 1992 to 1998 and a geochemical synthesis for the overall eruption. The dominant crustal magmatic processes are fractionation and accumulation of olivine, which caused short-term (days to weeks) compositional variations. Magma mixing was important only during the early part of the eruption and during episode 54. The overall systematic decrease in MgO-normalized CaO content and abundances of highly incompatible elements, without significant Pb, Sr and Nd isotope compositional variation, is interpreted to be caused by mantle melting processes. Experimental results and modeling of trace element variations indicate that neither batch melting nor simple progressive melting can explain these compositional variations. Instead, a more complex progressive melting model is needed. This model involves two source components with the same isotopic composition, but one was melted $\sim$ 3% in the Hawaiian plume. The model results indicate that the amount of this depleted source component progressively increased during the eruption from 0 to $\sim$ 25%. Given the isotopic similarity of Pu'u 'O'o lavas to many lavas from Loihi Volcano and the small extent of prior melting to form the depleted source component, the melting region for Pu'u 'O'o magmas may partially overlap with that of the adjacent, younger volcano, Loihi.

*Corresponding author. Telephone: +1-808-956-6641. Fax: +1-808-956-5512. e-mail: garcia@soest.hawaii.edu
†Present address: Department of Terrestrial Magnetism, Carnegie Institution of Washington, Washington, DC 20015, USA.
Extended data set can be found at:
http://www.petrology.oupjournals.org

INTRODUCTION

The Pu'u 'O'o eruption is the longest-lived, best monitored (e.g. Wolfe *et al.*, 1988) and most voluminous historical eruption of Kilauea Volcano (Fig. 1). It started in January 1983 and, 17 years later, it is still continuing vigorously ($\sim$ 300 000 m^3/day). About $\sim$ 2 km^3 of basaltic lava (dense rock equivalent) have been erupted, which destroyed 181 homes and a National Park visitor center on the south flank of the volcano (total losses $\sim$ $60 million). We previously documented the petrologic history of lavas from episodes 1 to 49 of this eruption (1983 to early 1992) utilizing petrography, mineral and whole-rock geochemistry [electron microprobe, X-ray fluorescence (XRF) and inductively coupled plasma mass spectrometry (ICP-MS) analyses], and Pb, Sr, Nd and O isotopes supplemented with field observations and geophysical data (Garcia & Wolfe, 1988; Garcia *et al.*, 1989, 1992, 1996, 1998*a*). This paper chronicles the petrology and geochemistry (including ICP-MS trace element data, and Pb, Sr and Nd isotopic ratios) of Pu'u 'O'o lavas from episodes 50 to 55 (1992 to early 1998), a period when $\sim$ 0·9 km^3 of lava was produced. In addition, we present the results of a time-series analysis of the entire eruption, which provides a rare opportunity to document both crustal magmatic processes (e.g. crystal
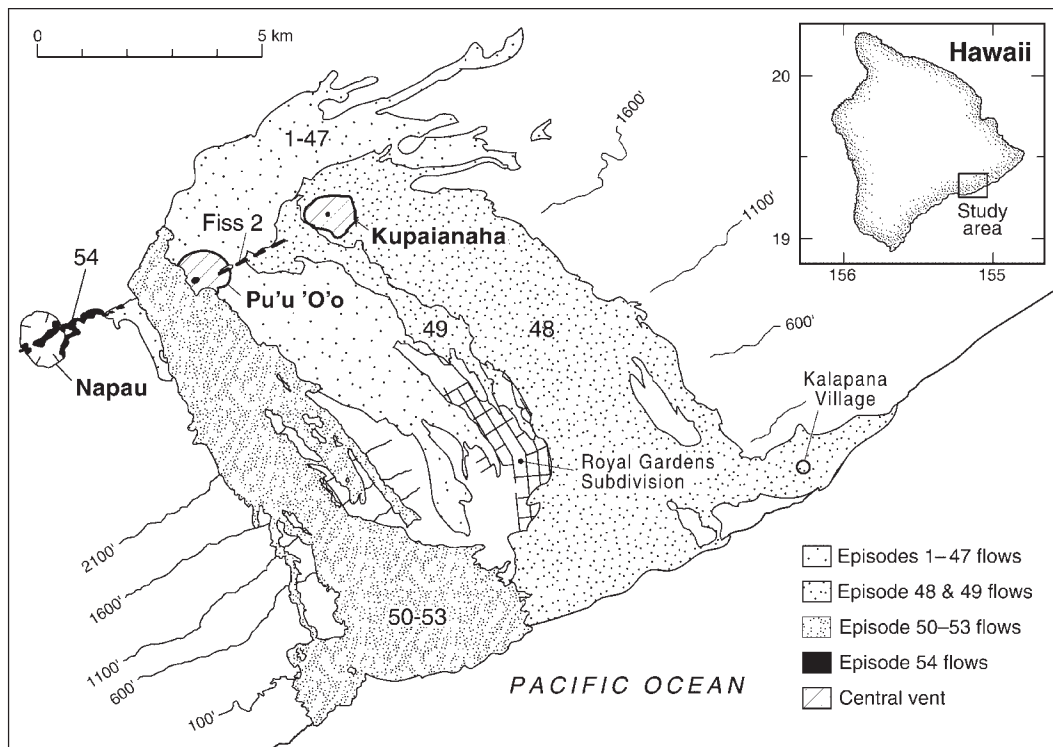
Fig. 1. Map of the Pu'u 'O'o eruption flow field on the east rift zone of Kilauea Volcano, Hawaii (after Heliker *et al.*, 1998*b*). Lava has erupted primarily from two central vents: Pu'u 'O'o (episodes 2–47, 50–53 and 55) and Kupaianaha (episode 48). A fissure system formed between these vents during episode 49 and uprift from the Pu'u 'O'o vent during episode 54. The lavas from the continuing episode 55 are not shown. The contour interval is 500 ft after the 100 ft contour (1 ft = 0·3048 m). The insert map shows the location of the eruption site on the island of Hawaii.

fractionation, magma mixing and crustal assimilation) and to investigate mantle melting systematics. In contrast to the brief, small-volume, historical eruptions (1790–1982; see Macdonald *et al.*, 1983), long-lived eruptions such as Pu'u 'O'o may have typified Kilauea's prehistoric history (e.g. Holcomb, 1987).

Our results show that olivine fractionation and accumulation are the dominant crustal processes during the Pu'u 'O'o eruption, although crustal assimilation and magma mixing have played important secondary roles during the early part of the eruption and during episode 54. A progressive change in whole-rock CaO concentration and in incompatible trace element abundances and ratios with essentially no change in Pb, Sr and Nd isotopic ratios indicates that mantle partial melting was the primary factor controlling compositional variation in Pu'u 'O'o lavas erupted from 1985 to 1998. Modeling of this compositional variation requires melting of an isotopically homogeneous source with a component that was previously melted ∼3%. The model results suggest that the proportion of this component in the lavas increased from 0 to ∼25% during the Pu'u 'O'o eruption. The isotopic similarity of Pu'u 'O'o lavas to many Loihi lavas, the small extent of previous melting of one of the source components, the southward dip of Kilauea's mantle conduit, and the indications from U-series data that Kilauea magmas are being derived from a large source area are all consistent with the possibility that these magmas were derived from the same source region that is supplying the adjacent, younger volcano, Loihi.

BRIEF HISTORY OF THE PU'U 'O'O ERUPTION

The character of the Pu'u 'O'o eruption has changed markedly during 17 years of activity (see Table 1 for a summary). Episode 1 involved a 'curtain of fire' along a discontinuous fissure system of 8 km length, which was intermittently active for almost a month (Wolfe *et al.*, 1987). Episodes 2–47 (February 1983–June 1986) were short lived (5–100 h) with lava fountains of variable heights (10–400 m). These episodes were followed by repose periods of 8–65 days during which magma accumulated and fractionated in a shallow reservoir under the Pu'u 'O'o vent (Wolfe *et al.*, 1988; Hoffmann *et al.*, 1990; Garcia *et al.*, 1992). In July 1986, the site of effusive activity shifted 3 km down-rift from the 255-m-high Pu'u

Table 1: Summary of the Pu'u 'O'o eruption, 1983–1999

Episode	Episode start date	Repose length (days)	Episode length	Volume (10^6 m³)	Vent location	Eruption rate (10^3 m³/day)
1	Jan. 03, 1983	start	20 days	14	Fissure 1	—
2–47	Feb. 10, 1983	8–65	~3.5 years	371	Mostly Pu'u 'O'o	~300
48	July 20, 1986	24	~5.5 years	~500	Kupaianaha	~400–0.5
49	Nov. 08, 1987	none	18 days	11	Fissure 2	0.6
50	Feb. 17, 1992	11	15 days	3	Pu'u 'O'o flank	—
51	Mar. 07, 1992	4	161 days	32	Pu'u 'O'o flank	~300
52	Oct. 03, 1992	none	15 days	2	Pu'u 'O'o flank	~300
53	Feb. 20, 1993	none	~4 years	~535	Pu'u 'O'o flank	~300
54	Jan. 30, 1997	none	~1 day	0.3	Fissure 3	0.3
55	Feb. 24, 1997	24	continuing	~265*	Pu'u 'O'o and its flank	200–500

Repose length refers to the duration of the pause between eruptive episodes; volume is the dense rock equivalent erupted during each episode. Vent locations (see Fig. 1): fissure 1—a discontinuous fissure system of 8 km length extending east from Napau crater under the Pu'u 'O'o cone; fissure 2—a discontinuous fissure system of 2 km length between the Pu'u 'O'o and Kupaianaha vents; Pu'u 'O'o flank—lava rose up in the throat of Pu'u 'O'o vent and drained onto the flow field through vents on the south flank of Pu'u 'O'o for episodes 52 and 55 and west flank for episodes 50, 51, 53 and 55; fissure 3—a discontinuous fissure of 2 km length extending from the west wall of Napau Crater eastward towards Pu'u 'O'o. Data sources: Episodes 1–20, Wolfe *et al.* (1988); episodes 21–47, Ulrich *et al.* (1987); episode 48, Kauahikaua *et al.* (1996); episode 49, Mangan *et al.* (1995); episodes 50–53, Heliker *et al.* (1998*b*); episode 54, Harris *et al.* (1997); episode 55, Heliker *et al.* (1998*a*). The eruption rate values are longer-term averages for each episode except episode 48, which showed a decrease from 250 000 m³/day to 54 000 m³/day during the 8 months before the Kupaianaha vent died; the values for episodes 51–53 are an average for only the period Nov. 1992–Feb. 1994.
*Estimated value as of January 1999.

'O'o cone to form the Kupaianaha vent (Fig. 1). Magma rose up in the throat of the Pu'u 'O'o cone and degassed vigorously before passing through a shallow underground channel to the Kupaianaha vent (Garcia *et al.*, 1996). This shift in the vent site marked a fundamental change in eruption style from episodic, high fountaining to nearly continuous, quiescent effusion. The Kupaianaha vent was active for 5·5 years during which it produced ~0·5 km³ of lava (dense rock equivalent) and built a shield of 56 m height during this 48th episode of the Pu'u 'O'o eruption (Kauahikaua *et al.*, 1996). Three months before the end of episode 48, a discontinuous fissure system of 1·7 km length opened up between the Pu'u 'O'o and Kupaianaha vents (episode 49). For approximately 21 days, this vent system produced lavas of the same composition as coeval lavas from the Kupaianaha vent (Garcia *et al.*, 1996). Activity at the Kupaianaha vent diminished during episode 49 and ended 2 months later.

With the demise of the Kupaianaha vent in early 1992, effusive activity resumed 11 days later at Pu'u 'O'o from vents on its flanks. Episode 50 was short lived (15 days) but the eruption restarted (episode 51) along the same fissure after a 4 day hiatus (Table 1). Episode 51 was interrupted by 17 short pauses (8–90 h) and ended ~7 months later following a magnitude 4·5 earthquake

near Pu'u 'O'o (Heliker *et al.*, 1998*b*). The next day, episode 52 began from two new vents on the southwest flank of the cone, ~200–300 m from the episode 51 vent (which resumed erupting the next day). Episode 52 continued until a seismic swarm and a rapid summit deflation in February 1993 (Heliker *et al.*, 1998*b*). Episode 53 started 9 days later and continued for almost 4 years until the Pu'u 'O'o lava lake suddenly drained and the cone collapsed on January 29, 1997. A few hours later, a 1 day eruption (episode 54) occurred along a discontinuous fissure system of 2 km length, 2–4 km up-rift from Pu'u 'O'o. Lava was produced during episode 54 from six, low fountaining (10–30 m high) vents (Harris *et al.*, 1997). A 24 day hiatus followed episode 54. During this period, no lava was observed in or near the Pu'u 'O'o cone and many volcano watchers thought the eruption was finally over. This eruption, however, is continuing (episode 55) and shows no signs of ending in the near future despite occasional short (1–4 day) eruptive pauses.

SAMPLES

Ninety-three lava samples representing episodes 50–53, six from episode 54 and an additional 29 from episode

55 were collected for this study. Whenever possible, samples were collected in a molten state from active lava flows and water-quenched to minimize post-eruptive crystallization. The episode 54 samples were collected several weeks after their eruption, but from rapidly quenched vent deposits and are labeled according to their eruptive vent (A–F). All other samples are labeled with the date that they were collected (day-month-year), which is probably within a day of their eruption. During episodes 50–52, lava samples were mostly collected within 100 m of the eruptive vent. Following the onset of episode 53, lava drained directly into tubes and only rarely were overflows and skylights available for sampling. Therefore, most of our samples from episode 53 and all from episode 55 were collected on the coastal plain, 10–12 km from the Pu'u 'O'o vent, as the lava discharged from lava tubes. Splits of our Pu'u 'O'o samples are available to anyone interested in performing additional analyses.

PETROGRAPHY

Episode 50–53 and 55 lavas, like the vast majority of other Pu'u 'O'o lavas we have studied, are glassy, strongly vesicular, friable and weakly to moderately olivine-phyric (0·4–6·2 vol. % phenocrysts; Table 2). Olivine is the only phenocryst in these samples; it is usually small ($\sim$0·1–1 mm in diameter), euhedral, undeformed and contains spinel and glass inclusions. Olivine is somewhat more common ($\sim$1 vol. %) in these lavas compared with those from the preceding 5·5 years of eruptive activity at the Kupaianaha vent (episode 48), despite identical ranges in MgO contents (7–10 wt %; Garcia *et al.*, 1996) for the lavas from the two periods. Olivine abundance in episodes 50–53 and 55 lavas is generally correlated positively with whole-rock *mg*-number, although olivine phenocryst abundance can vary as much as 5 vol. % for a given *mg*-number (Table 2).

Clinopyroxene (cpx) microphenocrysts occur in $\sim$65% of the episode 50–53 lavas and in many of the early episode 55 lavas that we examined but always in low abundance (<1·7 vol. %). Commonly, these small (0·1–0·3 mm) crystals occur in clusters of 3–12 grains and some have sector zoning. Plagioclase microphenocrysts (0·1–0·5 mm) are absent in the episode 50–52 samples we examined but rare (≤0·4 vol. %) crystals occur in $\sim$33% of the episode 53 samples. Tiny crystals (<0·1 mm) of plagioclase, olivine, spinel and clinopyroxene occur in a matrix of honey brown glass or black cryptocrystalline material in nearly all samples. Episode 55 samples collected after April 21, 1997, when surface activity became more vigorous, do not contain cpx or plagioclase microphenocrysts.

The episode 54 lavas are among the most aphyric samples from the Pu'u 'O'o eruption. They contain only

rare (≤0·2 vol. %) phenocrysts of olivine and plagioclase. Rare microphenocrysts of plagioclase, olivine and clinopyroxene are also present in these lavas.

Xenoliths are rarely reported in Kilauea lavas but are present in six of the samples we studied in thin section. These small basalt xenoliths contain 'black' olivine. Black olivines are created by high-temperature oxidation as forsteritic olivine (>90%), magnetite and hypersthene replace the original olivine (Macdonald, 1944).

MINERAL CHEMISTRY

Olivine and clinopyroxene compositions were determined for a suite of episode 50–55 lavas that span nearly the entire range of whole-rock MgO contents (6·1–10·1 wt %). Plagioclase compositions were determined for the two episode 54 lavas with plagioclase phenocrysts. The University of Hawaii, five-spectrometer, Cameca SX-50 electron microprobe with SAMx automation was used for the mineral analyses. Operating conditions were 15 kV, a minimum spot size of 1 μm and a beam current of 20 nA for olivine and pyroxene, and 10 nA for plagioclase. Each element was counted for 30–45 s on the peak and 15 s on the background. Concentrations were determined using a ZAF–PAP correction scheme. Analytical error is estimated to be $\sim$0·2% forsterite, and 1–2% relative for major elements and 5–10% relative for minor elements (<1 wt %) based on repeated analyses of standards. Three spot analyses were made in the core and one on the rim of each crystal to check for compositional zoning.

Olivine

Over 200 olivine crystals were analyzed from 19 episode 50–55 lavas. Most of the analyzed olivine crystals are normally zoned with <3% variation in forsterite (Fo) from core to rim. The forsterite content of the olivine cores from the episode 50–53 and 55 lavas range from 79·7 to 84·4% (Table 3) with a few notable exceptions (e.g. black olivines with Fo >90%). Phenocrysts and microphenocrysts in episode 50–53 lavas overlap in composition (average Fo contents of $\sim$81·0%) and have somewhat lower Fo contents than the olivines from episode 48 lavas ($\sim$82·5% average; Garcia *et al.*, 1996). Olivines from episode 55 lavas have somewhat higher forsterite contents then episode 50–53 olivine (average 82·4%) and have a compositional distinction between phenocrysts and microphenocrysts (average 83·5 vs 81·7% Fo, respectively).

Cores of olivines from lavas with a wide range of *mg*-numbers (56–61) have olivine compositions in equilibrium with the bulk rock (Fig. 2). Many episode 50–53 and 55 lavas, especially those with higher *mg*-numbers, contain

Table 2: Modal mineralogy of representative lavas from episodes 50 to 55 of the Pu'u 'O'o eruption

Sample	*mg*-no.	Olivine		Clinopyroxene	Plagioclase		Matrix
		ph	mph	mph	ph	mph	
Episode 50							
19-Feb-92	61·1	2·4	3·4	<0·1	0·0	0·0	94·2
23-Feb-92	61·8	0·4	2·4	<0·1	0·0	0·0	97·2
Episode 51							
13-Jun-92	61·2	2·0	3·8	1·0	0·0	0·0	93·2
05-Oct-92	58·6	2·4	1·2	0·4	0·0	0·0	96·0
29-Dec-92*	59·7	2·0	2·8	0·2	0·0	0·0	95·0
Episode 52							
04-Oct-92	60·8	1·6	3·2	1·6	0·0	0·0	93·6
Episode 53							
18-Mar-93*	60·2	2·2	3·2	0·2	0·0	0·0	94·4
16-Apr-93	60·1	1·2	2·2	0·0	0·0	0·0	96·6
09-May-93	61·1	1·8	2·8	0·0	0·0	0·0	95·4
30-Oct-93	56·5	0·6	1·0	0·2	0·0	0·4	97·8
14-Dec-93	60·2	0·8	2·0	1·4	0·0	0·0	95·8
13-Mar-94	59·1	0·8	2·2	0·4	0·0	0·0	96·6
18-May-94	57·5	2·4	3·2	1·6	0·0	<0·1	92·8
09-Oct-94	59·0	2·0	3·0	0·6	0·0	0·0	94·4
14-Jan-95*	59·0	2·4	3·0	1·4	0·0	0·0	93·2
29-Mar-95	58·4	1·6	2·2	0·4	0·0	0·0	95·8
14-Jun-95	61·3	3·6	2·6	0·6	0·0	0·0	93·2
11-Sep-95*	56·1	0·8	2·0	0·2	0·0	0·0	97·0
14-Oct-95*	60·5	2·6	3·8	0·4	0·0	0·4	92·8
19-Jan-96	63·4	6·2	2·4	0·6	0·0	0·2	90·6
15-Mar-96	59·2	2·8	5·0	0·2	0·0	<0·1	92·0
07-Jun-96	58·0	2·6	1·8	<0·1	0·0	<0·1	95·6
22-Aug-96	59·2	2·6	2·6	0·0	0·0	0·0	94·8
10-Jan-97	59·5	2·2	3·0	0·0	0·0	0·0	94·8
Episode 54							
B vent	51·7	<0·1	<0·1	0·2	0·0	0·4	99·4
D vent	52·4	<0·1	<0·1	<0·1	0·2	0·6	99·2
F vent	51·9	0·0	<0·1	0·4	0·0	1·6	98·0
Episode 55							
21-Apr-97	56·7	0·6	1·8	0·6	0·0	0·2	96·8
10-Aug-97*	62·9	5·0	5·4	0·0	0·0	0·0	89·6
11-Oct-97	58·0	0·8	1·0	0·0	0·0	0·0	98·2
26-Dec-97	61·6	2·6	3·4	0·0	0·0	0·0	94·0
10-Jan-98	61·3	1·8	4·4	0·0	0·0	0·0	93·8
27-Mar-98	60·6	3·2	2·2	0·0	0·0	0·0	94·6
10-Apr-98	61·3	1·4	4·2	0·0	0·0	0·0	94·4
11-May-98	60·8	5·2	3·0	0·0	0·0	0·0	91·8
17-Aug-98	60·8	1·4	3·4	0·0	0·0	0·0	95·2

mg-no. is [Mg/(Mg + Fe^{2+}) × 100], assuming Fe^{2+} = 0·9 of total iron. All values are in vol. % and are based on 500 point counts/sample. Phenocrysts (ph) are >0·5 mm across; microphenocrysts (mph) are 0·1–0·5 mm across. Matrix consists of glass and crystals <0·1 mm across.
*Contains black olivine in basalt xenolith(s).

Table 3: Representative microprobe analyses of olivines from episode 50–55 lavas of the Pu'u 'O'o eruption

Block 1

Episode:	50	50	50	51	51	51	51	51	52	52
Sample:	23-Feb-92	23-Feb-92	23-Feb-92	29-Dec-92	29-Dec-92	13-Jun-92	13-Jun-92	13-Jun-92	04-Oct-92	04-Oct-92
Rock *mg*-no.:	61.8	61.8	61.8	59.7	59.7	61.2	61.2	61.2	60.8	60.8
Size:	mph	mph	mph	ph-c	mph	ph-c	ph-c	mph	ph-c	mph
SiO$_2$	39.55	39.35	39.15	39.4	38.75	39.25	39.2	39.0	39.45	39.15
FeO	15.95	17.0	17.6	17.0	18.1	17.4	18.1	18.2	16.55	17.50
NiO	0.11	0.18	0.15	0.20	0.17	0.23	0.20	0.19	0.22	0.21
MgO	43.75	43.45	42.80	43.60	43.0	42.8	42.55	42.65	43.95	42.70
CaO	0.29	0.27	0.30	0.27	0.31	0.27	0.27	0.27	0.26	0.24
Total	99.65	100.25	100.00	100.47	100.3	99.95	100.32	100.31	100.43	99.8
Fo mol %	83.0	82.0	81.3	82.1	81.0	81.4	80.7	80.7	82.5	81.3

Block 2

Episode:	53	53	53	53	53	53	53	53	53	53	53
Sample:	18-Mar-93	18-Mar-93	09-May-93	09-May-93	09-May-93	13-Mar-94	13-Mar-94	13-Mar-94	29-Mar-95	29-Mar-95	29-Mar-95
Rock *mg*-no.:	60.2	60.2	61.1	61.1	61.1	59.1	59.1	59.1	58.4	58.4	58.4
Size:	bk ph-c	bk mph	ph-c	ph-r	mph	ph-c	ph-r	mph	ph-c	ph-r	mph
SiO$_2$	42.8	42.6	39.25	39.15	38.5	39.25	39.3	39.3	39.4	38.4	39.2
FeO	2.4	2.85	16.45	17.7	17.55	17.85	18.0	18.0	17.4	19.95	18.5
NiO	0.21	0.12	0.24	0.17	0.17	0.17	0.15	0.18	0.22	0.15	0.18
MgO	54.95	54.1	43.95	43.1	43.0	42.2	42.3	42.3	43.0	40.6	42.2
CaO	0.13	0.21	0.25	0.28	0.30	0.28	0.27	0.27	0.26	0.32	0.26
Total	100.49	99.88	100.14	100.4	99.52	99.75	100.02	100.05	100.28	99.42	100.34
Fo mol %	97.4	96.9	82.6	80.5	81.3	80.8	80.7	80.7	81.5	78.4	80.3

Block 3

Episode:	54	54	54	54	55	55	55	55	55
Sample:	B vent	B vent	D vent	D vent	10-Aug-97	11-May-98	11-May-98	11-May-98	11-May-98
Rock *mg*-no.:	51.7	51.7	52.4	52.4	62.9	60.8	60.8	60.8	60.8
Size:	mph	mph	mph	mph	bk mph	ph-c	xeno	ph-c	mph
SiO$_2$	39.75	40.2	40.3	38.9	41.5	39.3	38.9	39.6	39.8
FeO	16.1	13.9	13.7	19.3	4.7	16.85	21.75	16.0	16.9
NiO	0.20	0.26	0.23	0.01	0.19	0.18	0.14	0.26	0.23
MgO	43.0	44.65	44.85	40.1	53.0	42.8	39.2	43.7	42.3
CaO	0.25	0.25	0.25	0.27	0.15	0.26	0.25	0.25	0.48
Total	99.3	99.26	99.33	99.58	99.55	99.44	100.24	99.85	99.71
Fo mol %	82.6	85.1	85.3	78.8	90.2	81.6	76.0	82.7	81.2

Rock *mg*-no. is whole-rock [Mg/(Fe^{2+} + Mg)] × 100 assuming 90% of the total iron is Fe^{2+}; ph, phenocrysts; mph, microphenocrysts; c, core; r, rim; bk, black olivine; xeno, xenocryst. All oxide concentrations are in wt %.
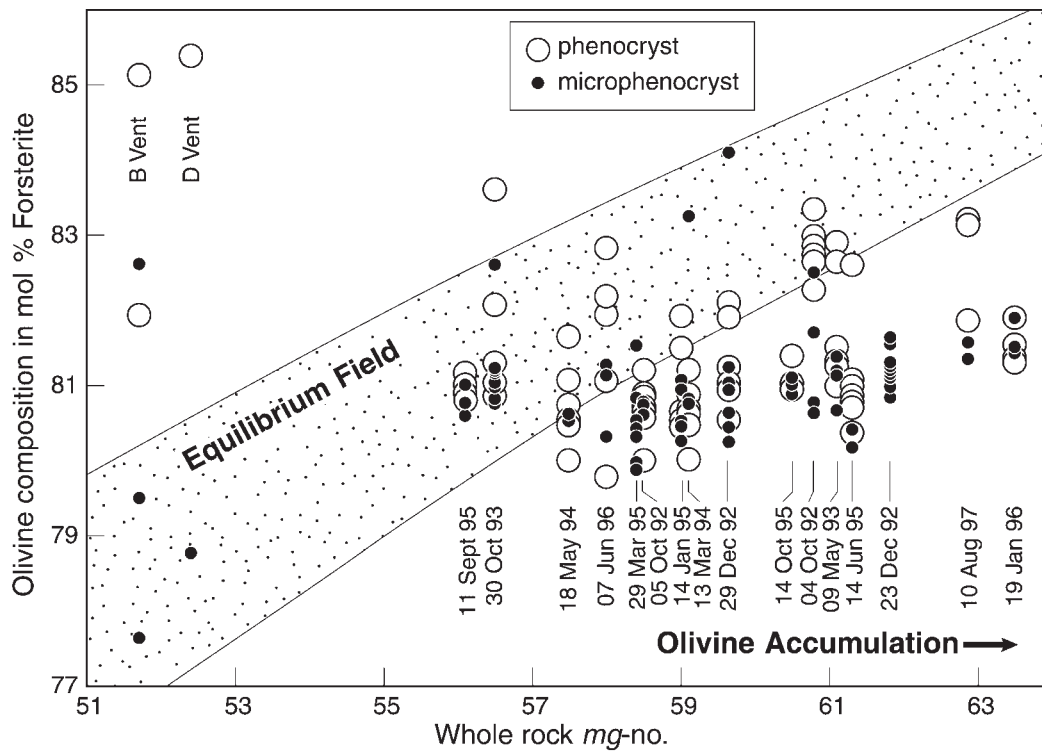
Fig. 2. Whole-rock *mg*-number [(Mg/(Mg + Fe^{2+}) × 100] vs olivine composition in forsterite content (Fo %) for crystal cores from episode 50–55 lavas. For the *mg*-number calculation, 90% of the total iron is assumed to be Fe^{2+} based on iron redox determinations of Hawaiian tholeiites (Moore & Ault, 1965). ○, phenocrysts (0·5–2 mm in diameter); ●, microphenocrysts (0·1–0·5 mm). The date below each vertical set of olivine data is the sample number. The diagonal stippled field is the low-pressure equilibrium field for basaltic magma (Fe/Mg K_d = 0·30 ± 0·03; Roeder & Emslie, 1970; Ulmer, 1989). Many of the olivines plot below the equilibrium field, especially for the lavas with higher *mg*-numbers, and so probably experienced olivine accumulation. The lavas from episode 54 (B and D vents) have the lowest *mg*-number but the largest range in forsterite content. This large Fo range is probably the result of magma mixing.

olivines with forsterite contents too low to be in equilibrium with melts corresponding to their whole-rock composition (Fig. 2). The olivines in these rocks are identical in appearance to those in Pu'u 'O'o lavas with lower *mg*-numbers. The positive correlation between olivine abundance and *mg*-number in Pu'u 'O'o lavas (Table 2) indicates that these lavas probably accumulated olivine. Sample 11-May-98 contains olivine crystals with forsterite contents up to ∼89%, which are too high to be in equilibrium with the host rock *mg*-number. These high-Fo crystals show no signs of deformation and are probably relics from a Pu'u 'O'o parental magma.

Episode 54 olivines are more variable in composition, with cores ranging from 78 to 85% Fo. Most of the rare olivines in these lavas are too forsteritic to be in equilibrium with the differentiated composition of their host rock (Fig. 2), although they are strongly zoned with rims in equilibrium with their bulk composition. These high-Fo olivines were probably derived from a more MgO-rich magma shortly before eruption.

The black olivines in the basalt xenoliths from episode 51 and 53 lavas have some of the highest forsterite contents ever reported for Hawaiian rocks (up to 97·6%; Table 3).

Clinopyroxene

Compositions were determined for ∼70 cpx crystals in 12 lavas from episodes 53 and 54 (Table 4). The crystals are compositionally unzoned or weakly normally zoned. Microphenocryst compositions in these lavas range in cpx end-member components from 10 to 17% ferrosilite, 28 to 43% wollastonite and 47 to 53% enstatite. Matrix crystals have a wider range in iron content (e.g. 8–24% ferrosilite). Cr$_2$O$_3$ contents of Pu'u 'O'o cpx are from 0·1 to 1·3 wt %, Al$_2$O$_3$ contents range from 1·3 to 3·8 wt % and Na$_2$O and TiO$_2$ contents are low (<0·25 wt % and <1·5 wt %). These compositions are typical of cpx from Hawaiian tholeiites (Fodor *et al.*, 1975). Many of the cpx crystals have low and variable CaO contents (e.g. 14·1–19·1 wt % for rim to core) but nearly constant *mg*-numbers (80·4–81·1; Table 4). These features are indicative of disequilibrium growth (see Lofgren, 1980).

Disequilibrium cpx was also noted in the early, evolved Pu'u 'O'o lavas but its presence was ascribed to magma mixing (Garcia *et al.*, 1992). No petrographic or mineral chemical evidence for magma mixing was observed in the episode 50–53 and 55 lavas.

Plagioclase

Compositions were determined for phenocrysts and microphenocrysts in two episode 54 D vent samples (Table 5), which are the only Pu'u 'O'o lavas we have sampled since episode 3 to contain plagioclase phenocrysts. These plagioclase crystals are strongly reversely zoned (7–8% anorthite) from core to near the rim ($\sim 30\,\mu m$) but are normally zoned at the rim.

WHOLE-ROCK GEOCHEMISTRY
XRF major and trace element analyses

Ninety-two samples from episode 50–55 lavas (~ 1.2 samples/month over a ~ 6.7 year period) were analyzed by XRF spectrometry in duplicate at the University of Massachusetts for major and trace elements (Rb, Sr, Y, Nb, Zr, Zn, Ni, Cr and V; Table 6). For details of the methods used and for analytical precision estimates, the reader is referred to Rhodes (1996). With these new analyses, our XRF dataset for Pu'u 'O'o lavas includes 395 samples (a full dataset of these analyses is available on the *Journal of Petrology* Web page, at http://www.petrology.oupjournals.org).

The lavas from episodes 50 to 55 extend the compositional range for the Pu'u 'O'o eruption (Fig. 3). A lava from episode 53 (19-Jan-96) is the most MgO rich of any Pu'u 'O'o lava (10.1 wt %) and an episode 54 lava (Vent F) has the lowest MgO (5.6 wt %). Overall, the episode 50–55 lavas are similar in composition to the other Pu'u 'O'o lavas, especially for Al_2O_3. In detail, the K_2O and CaO trends are offset to lower values, with the episode 55 lavas having the lowest values. Also, the K_2O–MgO trend is linear for episode 50–53 and 55 lavas compared with the curved trend observed for the earlier episodes of the eruption and expected from crystal fractionation (Fig. 3). This linear trend is probably related to mantle melting processes, which are discussed below. The episode 54 lavas are petrographically and geochemically similar to lavas from episodes 1 to 3 with low MgO contents (5.6–6.3 wt %) and are readily distinguished from other Pu'u 'O'o lavas by their relatively low CaO/Al_2O_3 (<0.78 vs >0.82).

Cr, Ni and Zn are compatible trace elements in the episode 50–55 Pu'u 'O'o lavas (Table 5). Cr and Ni show the most variation of any element in Pu'u 'O'o lavas (factors of 6.4 and 3.3, respectively). Plots of these elements relative to a highly incompatible element (e.g. K) define steep negative trends for episode 50–53 and 55 lavas that overlap with and extend beyond the field for older Pu'u 'O'o lavas (Fig. 4). There is a systematic decrease in K at a given Ni abundance indicating a progressive variation in parental magma composition during the eruption. Among the incompatible trace elements, Rb and Nb varied by a factor of two for episode 50–55 lavas, with less variation for Zr (1.65), Y (1.45), Sr (1.4) and V (1.3). Element–element and element-ratio plots of the highly incompatible elements demonstrate that the episode 50–53 and 55 lavas overlap in composition with previous Pu'u 'O'o lavas and thus were derived from compositionally similar mantle sources. The episode 54 lavas are similar to early Pu'u 'O'o lavas in Cr and Sr but have distinctly lower Ni and Nb for their K concentration (Fig. 4). These differences indicate that the episode 54 lavas are probably not related to the same batch of magma that was tapped during episodes 1–3 despite the close spatial relationships of their vents. The relatively small Sr variation (Table 5) and the decrease in Al_2O_3 with decreasing MgO for the most evolved rocks, especially episode 54 lavas (Fig. 3), indicates that the evolved lavas underwent plagioclase fractionation.

ICP-MS analyses

Twenty-eight samples from episodes 50 to 55 were analyzed for trace elements by ICP-MS in the same laboratory (Washington State University; Table 7) as the 32 lavas from episodes 1 to 48 (Garcia *et al.*, 1996). For a summary of the methods used, the reader is referred to King *et al.* (1993) and Pietruszka & Garcia (1999a). The analytical precision (1σ) is estimated to be 1–3% based on repeated analyses of a Kilauea basalt standard [Kil1919; for information on this standard, see Rhodes (1996) for XRF data and Pietruszka & Garcia (1999a) for ICP-MS data]. Plots of highly incompatible elements show excellent linear trends for the overall Pu'u 'O'o suite with the episode 50–55 lavas extending the range of the suite to both significantly higher and lower concentrations (Fig. 5). Plots of ratios of highly over moderately incompatible elements vs highly incompatible elements (e.g. La/Yb vs Ba) show an overall linear trend with the scatter reflecting variable amounts of crystal fractionation. The episode 54 lavas have distinctly higher La/Yb ratios compared with all previously analyzed Pu'u 'O'o lavas except for an episode 1 lava (Fig. 5). On ratio–ratio plots of highly incompatible elements (with the most incompatible element in the numerator; e.g. Ba/Ce and La/Ce) the episode 50–53 and 55 lavas form fields that overlap with the field for episode 1–48 lavas but extend to lower values for the more recent lavas (1995–1998; Fig. 5). The overall decrease in La/Yb with

Table 4: Representative microprobe analyses of clinopyroxenes in Puʾu ʾOʾo lavas from episodes 53 and 54

| Episode: | 53 | | | | 53 | | 53 | 53 | | | 53 | 54 |
| Sample: | 9-May-93 | | | | 18-May-94 | | 29-Mar-95 | 14-Jun-95 | | | 14-Oct-95 | D vent |
	mph-c	mph-r	mph-c	mph-r	mph-c	mph-c	mph-c	mph-c	mph-r	matrix	mph-c	matrix
SiO_2	51.34	53.59	51.92	50.43	52.47	51.38	52.63	52.45	51.75	50.35	52.69	51.35
TiO_2	0.92	0.52	0.91	1.30	0.54	0.86	0.58	0.62	0.80	1.48	0.54	1.18
Al_2O_3	2.65	1.32	2.26	3.19	2.28	3.32	2.03	2.13	2.71	3.79	1.94	3.38
Cr_2O_3	0.24	0.11	0.20	0.17	0.80	1.09	0.74	0.74	1.01	0.53	0.74	0.32
FeO	7.49	8.64	8.05	8.88	6.24	6.25	6.21	6.44	6.54	7.70	6.29	8.18
MnO	0.16	0.19	0.17	0.19	0.33	0.22	—	0.18	0.17	0.19	—	—
MgO	17.26	20.81	17.69	17.61	17.98	16.68	17.63	18.12	17.10	15.83	17.96	17.63
CaO	19.14	14.09	18.08	17.30	18.64	19.62	19.71	19.28	19.33	19.29	18.88	16.86
Na_2O	0.40	0.54	0.37	0.46	0.22	0.24	0.21	0.22	0.20	0.23	0.20	0.19
Total	99.60	99.81	99.65	99.53	99.50	99.66	99.74	100.18	99.61	99.39	99.24	99.10
Pyroxene end members (mol %)												
En	49.0	58.1	50.2	50.3	51.5	48.6	50.3	50.9	50.9	46.5	51.2	51.3
Fs	11.9	13.5	12.8	14.2	10.0	10.2	9.3	10.2	10.2	12.7	10.1	13.4
Wo	39.1	28.3	36.9	35.5	38.4	41.1	40.4	38.9	38.9	40.8	38.7	35.4
mg-no.	80.4	81.1	79.7	77.9	83.7	82.6	83.5	83.4	82.3	78.6	83.6	79.3
Geothermobarmetry (Putrika et al., 1996)												
T (°C)	1212	1158	1206	1168	1190	1195	1196	1198	1209	1212	1210	1167
P (GPa)	0.60	−0.08	0.51	0.23	0.43	0.55	0.47	0.42	0.55	0.68	0.55	0.20

mph, microphenocrysts; c, core; r, rim; all oxide concentrations are in wt %; pyroxene *mg*-no. is [Mg/(Fe + Mg)] × 100.

Table 5: Microprobe analyses of plagioclase in two samples from vent D, episode 54

Sample type and size	Area	SiO_2	Al_2O_3	FeO	CaO	Na_2O	Total	An %
ph, 0·9 mm	core	52·51	30·09	0·75	12·93	4·00	100·28	64·1
	near rim	50·52	31·41	0·77	14·41	3·20	100·30	71·3
	rim	51·07	30·50	0·76	13·82	3·46	99·61	68·8
mph, 0·3 mm	core	50·42	31·57	0·65	14·49	3·30	100·43	70·8
	near rim	48·35	32·65	0·71	15·88	2·39	99·97	78·6
	rim	52·73	29·91	0·63	12·86	3·95	100·08	65·3

An %, mole per cent anorthite; ph, phenocryst; mph, microphenocryts.

time could be caused by an increase in the degree of partial melting during the eruption. The decrease in ratios of highly incompatible trace elements cannot be explained by an increase in partial melting and instead indicates that there was a minor change in the mantle source composition for the more recent lavas.

Pb, Sr and Nd isotopes

Ratios of Pb, Sr and Nd isotopes were determined on selected Pu'u 'O'o samples at the University of Hawaii using a VG Sector mass spectrometer [see Pietruszka & Garcia (1999*a*) for a summary of methods used]. Isotope fractionation corrections, standard values, total procedural blanks, and analytical uncertainties are given in Table 8. Five samples, one each from episodes 51 and 55, and three from 53, were analyzed for isotope ratios; the data for two of these samples (29-Dec-92 and 25-Apr-94) were presented by Garcia *et al.* (1996). Our previous work showed that Pb and Sr isotope ratios changed somewhat during the first 2 years of the eruption, a period of extensive magma mixing and crustal contamination (Garcia *et al.*, 1992, 1998*a*), but remained nearly constant for the next 7 years (Garcia *et al.*, 1996).

The new isotopic data for episode 51, 53 and 55 lavas show slight temporal increases in Pb and Sr isotope ratios, although the Sr isotope variation is essentially within analytical error (Fig. 6). Pu'u 'O'o lavas deviate from the good negative correlation observed for Pb and Sr isotope ratios in most Hawaiian tholeiites (e.g. West *et al.*, 1987), as do Loihi tholeiites (Fig. 7). The Pb and Sr isotopic data for tholeiites erupted during the last ~20 years from the three adjacent, active Hawaiian volcanoes are distinctly different (Fig. 7) and demonstrate that the Hawaiian plume source must have at least three distinct components [as suggested by Staudigel *et al.* (1984)]. Compared with other historical Kilauea lavas analyzed in the same laboratory (Pietruszka & Garcia,

1999*a*), Pu'u 'O'o lavas have the lowest $^{206}Pb/^{204}Pb$ ratios and plot within the Loihi field (Fig. 7). Nd isotope ratios have not varied beyond analytical error for the entire eruption (Garcia *et al.*, 1996; Table 7).

MAGMATIC CONDITIONS FOR THE PU'U 'O'O ERUPTION

The Pu'u 'O'o eruption provides an excellent opportunity to examine the details of magmatic processes at an active basaltic volcano because we have a wealth of background information on Kilauea's basic magmatic processes (e.g. Tilling & Dvorak, 1993). Seismic evidence has documented a vertical conduit of 60 km length that supplies magma to Kilauea (Tilling & Dvorak, 1993). For the Pu'u 'O'o eruption, magma in this conduit is thought to bypass the summit reservoir and feed directly into the east rift zone conduit (based on the rapid change in trace element geochemistry for Pu'u 'O'o lavas compared with Kilauea summit lavas; Garcia *et al.*, 1996). Seismic and ground deformation studies indicate that the east rift zone supplies a shallow (~0·5–2·5 km depth) magma reservoir under the Pu'u 'O'o vent (Koyanagi *et al.*, 1988; Hoffmann *et al.*, 1990; Gillard *et al.*, 1996). From 1983 to 1986, this reservoir was a narrow (~3 m wide), dike-like body (~1·6 km long and 2·5 km deep) that belched out much of its contents during brief (~1 day), monthly eruptions (Hoffmann *et al.*, 1990). The crown of the Pu'u 'O'o magma reservoir is open, which allows heat and gases to escape readily (Wolfe *et al.*, 1988). The high surface area and open top of this magma reservoir is thought to have caused rapid crystal fractionation (~5%) during the 20–30 day pauses between episodes 4–47 (Garcia *et al.*, 1992). There are no data to constrain the current size or shape of the Pu'u 'O'o reservoir since episode 47 but it is assumed to have remained small (e.g. Heliker *et al.*, 1998*b*). Its shape may have changed to a

Table 6: XRF whole-rock analyses of Pu'u 'O'o lavas from episodes 50 to 55

Sample	Day	SiO$_2$	TiO$_2$	Al$_2$O$_3$	Fe$_2$O$_3$	MnO	MgO	CaO	Na$_2$O	K$_2$O	P$_2$O$_5$	Total	Y	Sr	Rb	Nb	Zr	Ni	Cr	V	Zn
Episode 50																					
18-Feb-92	3333	49·78	2·370	12·79	12·40	0·17	8·75	10·59	2·14	0·414	0·223	99·63	24·1	317	6·8	12·9	151	167	521	291	112
19-Feb-92	3334	49·75	2·368	12·82	12·30	0·18	8·78	10·55	2·32	0·427	0·226	99·72	24·3	320	7·0	13·2	151	170	507	284	113
22-Feb-92	3337	49·75	2·335	12·67	12·45	0·17	9·30	10·45	2·18	0·411	0·221	99·94	24·4	315	6·5	13·1	151	171	539	289	129
23-Feb-92a	3338	49·76	2·338	12·71	12·44	0·17	9·16	10·47	2·21	0·409	0·221	99·89	24·3	315	6·7	13·0	147	185	557	289	118
23-Feb-92b	3338	49·52	2·325	12·63	12·37	0·17	9·09	10·42	2·17	0·496	0·230	99·42	24·0	313	6·9	12·7	147	184	567	281	134
Episode 51																					
12-Mar-92	3356	49·68	2·350	12·71	12·44	0·18	8·97	10·53	2·12	0·412	0·221	99·61	24·4	316	6·8	13·0	148	176	541	286	119
29-Mar-92	3373	49·88	2·366	12·84	12·43	0·17	8·76	10·59	2·23	0·423	0·224	99·91	—	—	—	13·1	148	167	517	282	116
05-Apr-92	3380	49·76	2·368	12·71	12·41	0·18	8·87	10·55	2·25	0·422	0·230	99·75	24·6	321	6·6	13·8	149	169	525	286	130
12-Apr-92	3387	49·65	2·351	12·64	12·36	0·18	8·99	10·48	2·13	0·421	0·230	99·43	23·9	318	6·9	13·8	147	178	544	284	161
27-Apr-92	3402	49·74	2·363	12·75	12·38	0·18	8·77	10·54	2·22	0·421	0·230	99·59	24·3	323	7·1	14·0	149	164	525	273	117
26-May-92	3431	49·58	2·339	12·65	12·54	0·18	9·04	10·51	2·07	0·413	0·220	99·54	24·1	315	7·0	13·8	147	176	546	275	117
06-Jun-92	3442	49·65	2·352	12·68	12·49	0·18	8·94	10·59	2·11	0·416	0·230	99·64	23·9	319	7·1	14·7	149	172	530	282	118
13-Jun-92	3449	49·63	2·345	12·68	12·37	0·18	8·86	10·53	2·20	0·419	0·230	99·44	24·3	318	7·1	13·9	151	173	522	283	134
16-Jun-92	3452	49·69	2·363	12·69	12·42	0·18	8·80	10·53	2·24	0·420	0·230	99·56	24·1	322	6·9	13·7	153	172	516	280	121
07-Jul-92	3473	49·76	2·386	12·85	12·34	0·18	8·51	10·59	2·27	0·424	0·230	99·54	24·6	319	7·1	13·7	152	162	484	287	121
27-Aug-92	3524	49·88	2·397	13·03	12·33	0·18	8·33	10·68	2·31	0·427	0·230	99·79	24·5	324	7·3	13·6	154	142	463	288	121
08-Sep-92	3536	49·88	2·364	12·84	12·36	0·18	8·62	10·54	2·27	0·420	0·230	99·70	24·4	320	6·6	13·4	151	157	484	285	121
05-Oct-92	3563	50·27	2·445	13·18	12·32	0·18	7·93	10·78	2·37	0·434	0·240	100·15	25·0	328	7·1	14·0	153	131	394	290	119
01-Nov-92	3590	49·69	2·341	12·60	12·46	0·18	9·09	10·51	2·24	0·426	0·220	99·76	24·1	315	6·7	12·6	144	174	515	279	117
07-Nov-92	3596	49·63	2·350	12·63	12·51	0·18	8·95	10·49	2·17	0·418	0·230	99·56	24·8	320	6·7	13·1	147	161	488	283	119
12-Nov-92	3601	49·81	2·387	12·82	12·38	0·18	8·52	10·61	2·20	0·423	0·230	99·56	24·6	320	7·5	13·1	146	160	482	284	135
29-Dec-92	3648	49·57	2·355	12·69	12·42	0·18	8·80	10·52	2·22	0·419	0·230	99·40	24·0	318	6·8	13·5	149	170	498	280	120
09-Jan-93	3659	49·81	2·373	12·84	12·40	0·18	8·57	10·63	2·29	0·423	0·230	99·75	24·3	320	7·0	13·3	149	147	474	283	364
Episode 52																					
04-Oct-92	3562	49·74	2·359	12·79	12·37	0·18	8·73	10·55	2·31	0·419	0·230	99·68	24·6	319	6·7	13·2	150	156	484	280	120
Episode 53																					
20-Feb-93	3701	50·00	2·404	12·97	12·45	0·18	8·37	10·71	2·26	0·415	0·232	99·99	24·4	317	7·2	13	150	132	452	282	120
18-Mar-93	3727	49·93	2·382	12·87	12·55	0·18	8·64	10·63	2·20	0·415	0·231	100·03	24·1	313	7·1	12·8	148	140	493	281	116
16-Apr-93	3756	49·86	2·379	12·85	12·49	0·17	8·56	10·64	2·14	0·413	0·231	99·73	24·1	313	7·1	12·8	148	143	501	284	116
09-May-93	3779	49·77	2·347	12·73	12·47	0·18	8·90	10·55	2·23	0·419	0·230	99·83	24·2	317	6·8	13·3	149	166	476	285	121
10-May-93	3780	49·91	2·303	12·80	12·49	0·18	8·62	10·64	2·20	0·409	0·227	99·83	25·1	319	6·5	13·9	149	151	504	282	117

Table 6: continued

Date	Day	SiO$_2$	TiO$_2$	Al$_2$O$_3$	Fe$_2$O$_3$	MnO	MgO	CaO	Na$_2$O	K$_2$O	P$_2$O$_5$	Total	Y	Sr	Rb	Nb	Zr	Ni	Cr	V	Zn
09-Jun-93	3810	49·78	2·370	12·76	12·48	0·18	8·58	10·62	2·28	0·488	0·231	99·77	24·3	314	7·3	12·9	148	139	490	284	116
08-Jul-93	3839	49·96	2·381	12·79	12·52	0·18	8·56	10·64	2·35	0·413	0·231	100·01	24·3	313	7·1	13·8	148	140	503	283	1134
13-Aug-93	3875	50·12	2·390	12·96	12·51	0·18	8·41	10·76	2·14	0·418	0·231	100·12	24·8	321	6·5	14·3	146	140	458	290	160
27-Sep-93	3920	50·15	2·379	12·96	12·47	0·18	8·40	10·75	2·09	0·417	0·232	100·03	24·8	321	7·2	14·6	144	135	453	289	116
30-Oct-93	3953	50·35	2·466	13·35	12·31	0·18	7·26	11·07	2·24	0·432	0·239	99·90	—	331	7·1	15·1	152	94	376	295	182
14-Dec-93	3998	49·87	2·388	12·99	12·41	0·18	8·19	10·79	2·36	0·420	0·230	99·83	24·7	319	6·7	13·8	154	130	441	295	120
04-Jan-94	4019	50·38	2·470	13·41	12·33	0·18	7·28	11·04	2·38	0·436	0·240	100·15	25·4	331	6·9	14·7	157	97	367	298	169
11-Feb-94	4057	50·02	2·402	13·04	12·45	0·18	8·15	10·82	2·31	0·424	0·230	100·03	25·0	323	7·1	14·3	157	119	439	297	119
13-Mar-94	4087	49·99	2·401	13·02	12·45	0·18	8·17	10·81	2·32	0·423	0·230	99·99	25·1	323	7·5	13·9	156	128	441	297	119
09-Apr-94	4114	50·38	2·440	13·26	12·40	0·18	7·80	10·92	2·41	0·427	0·240	100·46	25·3	326	7·6	13·8	158	110	409	304	118
11-Apr-94	4116	50·05	2·380	13·02	12·46	0·18	8·34	10·78	2·34	0·422	0·230	100·20	24·4	321	6·5	14·4	155	142	440	294	119
25-Apr-94	4130	50·16	2·441	13·27	12·42	0·18	7·71	10·93	2·45	0·429	0·240	100·23	25·7	329	6·6	14·1	156	107	379	300	120
18-May-94	4153	50·01	2·452	13·23	12·36	0·18	7·61	10·91	2·33	0·430	0·238	99·81	24·8	326	7·5	13·4	153	104	383	290	116
21-Jun-94	4187	50·20	2·437	13·33	12·42	0·18	7·89	10·93	2·39	0·430	0·240	100·45	24·9	326	7·6	13·9	157	127	414	296	146
11-Jul-94	4207	50·05	2·426	13·05	12·41	0·18	7·93	10·84	2·26	0·425	0·233	99·80	24·8	323	7·5	13·3	152	115	509	290	117
02-Aug-94	4229	49·99	2·434	13·13	12·40	0·18	7·72	10·85	2·36	0·433	0·240	99·74	24·9	314	7·4	13·2	153	109	396	285	117
25-Aug-94	4252	49·83	2·400	12·96	12·44	0·18	8·00	10·79	2·31	0·427	0·230	99·57	24·4	305	7·0	13·2	151	119	409	284	116
09-Oct-94	4297	49·82	2·386	12·91	12·51	0·18	8·19	10·72	2·23	0·409	0·230	99·59	25·5	325	7·1	14·1	150	124	428	292	120
16-Nov-94	4335	50·14	2·409	13·31	12·51	0·18	8·05	10·78	2·23	0·379	0·250	99·86	25·2	328	7·2	14·1	151	122	418	294	121
29-Dec-94	4378	50·02	2·415	13·00	12·51	0·18	8·03	10·74	2·28	0·418	0·240	99·83	24·8	326	6·9	14·7	152	119	410	292	120
14-Jan-95	4394	49·91	2·398	12·96	12·56	0·18	8·21	10·71	2·22	0·406	0·230	99·78	23·7	325	6·5	14·0	150	129	443	292	120
24-Feb-95	4435	50·15	2·432	13·14	12·50	0·18	7·87	10·80	2·17	0·423	0·233	99·90	25·2	325	7·4	14·2	152	120	412	295	119
29-Mar-95	4468	50·13	2·412	13·10	12·49	0·18	7·99	10·76	2·17	0·421	0·232	99·89	25·1	323	6·8	14·3	152	117	423	293	120
27-Apr-95	4497	49·92	2·374	12·91	12·57	0·18	8·40	10·63	2·15	0·411	0·230	99·78	24·5	319	6·8	14·4	148	131	455	287	118
13-Jun-95	4544	49·74	2·323	12·57	12·79	0·18	9·21	10·42	2·12	0·404	0·224	99·99	23·7	306	7·0	12·5	145	144	480	272	117
05-Jul-95	4566	49·87	2·403	12·98	12·46	0·18	7·97	10·73	2·65	0·504	0·233	99·48	24·5	317	7·2	12·7	150	109	415	282	116
15-Aug-95	4607	49·87	2·375	12·90	12·56	0·18	8·32	10·64	2·06	0·412	0·226	99·54	24·4	314	7·2	12·7	149	125	453	284	117
11-Sep-95	4634	50·39	2·460	13·40	12·30	0·18	7·15	11·04	2·17	0·427	0·234	99·75	24·8	323	7·3	12·9	152	84	382	288	115
14-Oct-95	4667	49·61	2·336	12·63	12·82	0·19	8·94	10·38	1·95	0·406	0·223	99·49	23·8	307	6·9	12·5	146	146	446	177	118
19-Jan-96	4764	49·32	2·234	12·17	12·90	0·18	10·14	10·05	1·87	0·386	0·214	99·48	23·0	294	6·6	11·9	139	183	568	266	117
19-Feb-96	4795	50·02	2·373	12·95	12·48	0·18	8·14	10·71	2·04	0·407	0·226	99·54	24·4	311	6·8	12·6	147	118	451	284	117
15-Mar-96	4820	49·99	2·356	12·84	12·53	0·18	8·27	10·64	2·07	0·417	0·224	99·52	24·2	310	6·9	12·5	147	121	453	282	117
07-Jun-96	4904	50·50	2·405	13·35	12·35	0·19	7·75	10·91	2·21	0·413	0·229	100·30	24·4	316	7·8	12·5	149	81	366	283	114
22-Aug-96	4980	50·15	2·369	13·03	12·49	0·19	8·23	10·76	2·24	0·407	0·225	100·08	24·1	309	7·2	12·2	146	108	411	280	115
10-Jan-97	5121	50·10	2·349	12·98	12·46	0·19	8·33	10·74	2·08	0·402	0·220	99·86	23·9	307	7·0	12·2	143	125	468	284	125
26-Jan-97	5137	50·18	2·305	12·74	12·48	0·18	9·03	10·49	2·21	0·403	0·218	100·24	23·4	299	7·0	12	140	145	523	274	114
30-Jan-97	5141	49·85	2·343	12·91	12·48	0·19	8·32	10·71	2·16	0·404	0·220	99·59	24·6	313	7·2	12·9	146	93	387	288	119
30-Jan-97	5141	50·45	2·422	13·31	12·33	0·19	7·53	10·98	2·24	0·418	0·230	100·10	24·7	314	7·0	12·5	146	96	377	280	114

Date	Day	SiO$_2$	TiO$_2$	Al$_2$O$_3$	Fe$_2$O$_3$	MnO	MgO	CaO	Na$_2$O	K$_2$O	P$_2$O$_5$	Total	Y	Sr	Rb	Nb	Zr	Ni	Cr	V	Zn
Episode 54																					
Vent A	5141	50·21	2·960	13·62	12·63	0·19	6·37	10·35	2·38	0·588	0·310	99·61	28·5	376	10·6	18·7	194	82	154	320	125
Vent B	5141	50·18	2·995	13·66	12·62	0·19	6·15	10·34	2·47	0·604	0·320	99·52	28·7	382	10·7	19·0	197	77	114	319	125
Vent B2	5141	50·17	2·965	13·63	12·61	0·19	6·31	10·33	2·46	0·590	0·310	99·57	28·2	379	10·7	18·7	194	81	138	313	123
Vent D	5141	50·41	2·933	13·79	12·54	0·19	6·30	10·43	2·47	0·635	0·310	100·01	28·2	375	10·4	18·3	191	79	128	317	124
Vent E	5141	50·15	2·970	13·72	12·61	0·19	6·22	10·35	2·49	0·594	0·310	99·61	28·5	378	10·7	18·7	195	79	130	322	124
Vent F	5141	50·90	3·443	13·50	13·16	0·18	5·61	9·63	2·62	0·723	0·391	100·16	33·6	388	13·2	23·3	238	68	88	349	133
Episode 55																					
04-Apr-97	5205	50·24	2·410	13·28	12·25	0·17	7·52	10·90	2·36	0·410	0·228	99·77	24·3	314	7·4	12·5	148	95	366	285	116
21-Apr-97	5222	50·34	2·404	13·29	12·38	0·19	7·55	10·93	2·19	0·416	0·230	99·92	24·7	314	7·0	12·5	146	96	377	280	114
25-May-97	5256	50·33	2·392	13·21	12·39	0·19	7·71	10·91	2·14	0·413	0·230	99·91	24·5	312	7·2	12·6	146	103	387	285	115
13-Jul-97	5305	50·14	2·354	13·08	12·38	0·19	7·92	10·85	2·15	0·404	0·220	99·69	24·3	309	6·7	12·4	143	101	377	276	115
23-Jul-97	5315	50·39	2·380	13·20	12·35	0·19	7·60	10·96	2·13	0·408	0·230	99·84	24·4	311	7·0	12·4	145	95	381	282	114
10-Aug-97	5333	49·56	2·245	12·42	12·72	0·18	9·84	10·17	2·26	0·385	0·212	99·99	22·9	293	6·8	11·7	138	177	528	267	116
11-Oct-97	5395	50·47	2·382	13·16	12·26	0·18	7·91	10·86	2·24	0·407	0·228	100·10	24·1	310	6·9	12·4	145	98	413	272	112
18-Oct-97	5402	50·19	2·307	12·85	12·57	0·18	8·89	10·53	2·21	0·394	0·220	100·34	23·2	299	6·7	11·8	140	147	521	262	112
26-Dec-97	5471	50·18	2·305	12·74	12·48	0·18	9·03	10·49	2·21	0·403	0·218	100·24	23·4	299	7·0	12	140	145	523	274	114
10-Jan-98	5486	50·16	2·299	12·83	12·48	0·18	8·99	10·47	2·10	0·393	0·218	100·12	23·4	299	6·6	11·8	140	150	540	274	321
17-Jan-98	5493	50·16	2·282	12·70	12·48	0·18	9·26	10·42	2·21	0·402	0·215	100·31	23·2	297	7·0	11·7	139	146	519	273	115
18-Jan-98 E	5494	50·20	2·291	12·77	12·49	0·18	8·98	10·41	2·15	0·394	0·219	100·06	23·1	297	6·9	11·7	140	155	548	273	114
18-Jan-98 S	5494	50·18	2·301	12·82	12·38	0·17	8·91	10·42	2·16	0·397	0·216	99·95	23·3	298	7·0	11·8	140	153	552	274	114
21-Jan-98	5497	50·66	2·371	13·24	12·24	0·17	7·96	10·82	2·21	0·412	0·224	100·31	24·1	307	7·1	12·1	143	109	454	275	113
27-Mar-98	5562	50·07	2·319	12·77	12·40	0·17	9·03	10·45	2·15	0·409	0·221	99·99	23·6	302	7·2	12·1	142	157	541	275	115
10-Apr-98	5576	50·09	2·326	12·78	12·41	0·17	8·94	10·47	2·11	0·400	0·221	99·92	23·5	303	7·1	12·2	143	147	520	275	113
11-May-98	5607	50·21	2·316	12·80	12·40	0·17	9·10	10·40	2·10	0·405	0·221	100·13	23·5	301	7·1	12·2	142	168	549	274	115
22-May-98	5618	50·29	2·358	12·97	12·31	0·17	8·56	10·59	2·19	0·411	0·225	100·07	24·0	306	7·2	12·4	144	138	490	278	115
17-Aug-98	5705	50·34	2·366	12·94	12·35	0·18	8·70	10·58	2·15	0·410	0·226	100·24	23·6	307	7·4	12·4	145	141	476	227	115
07-Sep-98	5726	50·26	2·353	12·98	12·32	0·17	8·65	10·58	2·24	0·406	0·224	100·16	23·7	306	7·5	12·4	145	145	493	278	115

Day is the number of days since the start of the Pu'u 'O'o eruption on Jan. 03, 1983. Oxide concentrations are in wt %; trace elements are in ppm.
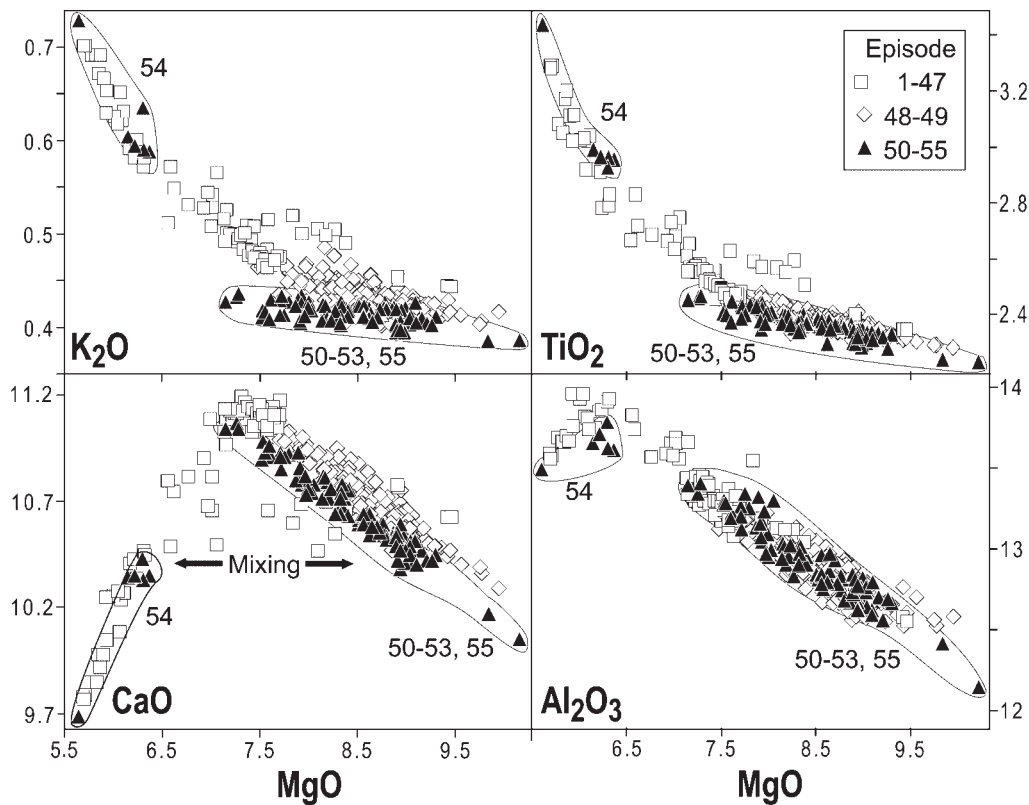
Fig. 3. Whole-rock MgO variation diagrams for lavas from episodes 1 to 55 of the Pu'u 'O'o eruption. The overall curved (K_2O, TiO_2) and kinked (Al_2O_3, CaO) trends indicate that crystal fractionation was a dominant process controlling compositional variation for most Pu'u 'O'o lavas. Some of the lavas from episodes 3 to 10 plot below the kink on the CaO diagram marking the onset of clinopyroxene fractionation. These lavas show petrographic signs of magma mixing (Garcia *et al.*, 1992). The scatter on these plots is greater than analytical error (the 2σ error is about symbol size), which indicates that the parental magma composition changed during the eruption. All values are in wt %. The two fields enclose the mafic lavas from episodes 50 to 53 and 55 and the evolved lavas from episode 54. The data are from Table 5 and Garcia *et al.* (1992, 1996).

more thermally efficient form with the change from episodic to continuous effusion in mid-1986.

The temperature of Pu'u 'O'o magma just before eruption can be inferred from the MgO contents of glasses (Helz & Thornber, 1987), clinopyroxene compositions (Putirka *et al.*, 1996) and from thermocouple measurements of molten lava. Temperatures of 1145–1160°C have been determined for Pu'u 'O'o glasses (Mangan *et al.*, 1995; Heliker *et al.*, 1998b), which agree well with measured lava temperatures (1135–1160°C). Temperatures calculated from cpx matrix and microphenocryst rim compositions yield similar to higher temperatures (1158–1212°C; Table 4). Cpx microphenocryst cores yield consistently high temperatures (1187–1212°C), which might be considered more representative of magmatic rather than eruption temperatures. Experiments on Kilauea lava compositions indicate that lower temperatures (1160–1172 $\pm$ 9°C) are more appropriate for low-pressure growth of cpx (Helz & Thornber, 1987).

Crystallization pressures for the Pu'u 'O'o reservoir can be inferred from several lines of evidence. Seismic and ground deformation studies indicates that the reservoir is shallow (<3 km depth) corresponding to pressures of <0·10 GPa (Hoffmann *et al.*, 1990). Thermobarometry calculations for cpx microphenocryst cores yield much higher pressures for episode 53 magmas ($\sim$0·51 $\pm$ 0·09 GPa; Table 4). Similar values were also reported for cpx microphenocrysts in lavas from episodes 9 and 10 (Putirka, 1997). Surprisingly, high pressures were also calculated for some matrix and microphenocryst rim compositions (0·55 and 0·68 GPa; Table 4). These mantle depth estimates (the Moho is $\sim$13 km, $\sim$4 GPa, at its deepest point under Kilauea; Klein *et al.*, 1987) are inconsistent with petrographic, field, experimental and geochemical evidence, which indicates that cpx forms late in Pu'u 'O'o lavas.

The liquidus mineralogy of a MgO-rich Pu'u 'O'o lava was modeled using the MELTS program (Ghiorso & Sack, 1995) to better understand the cause of the
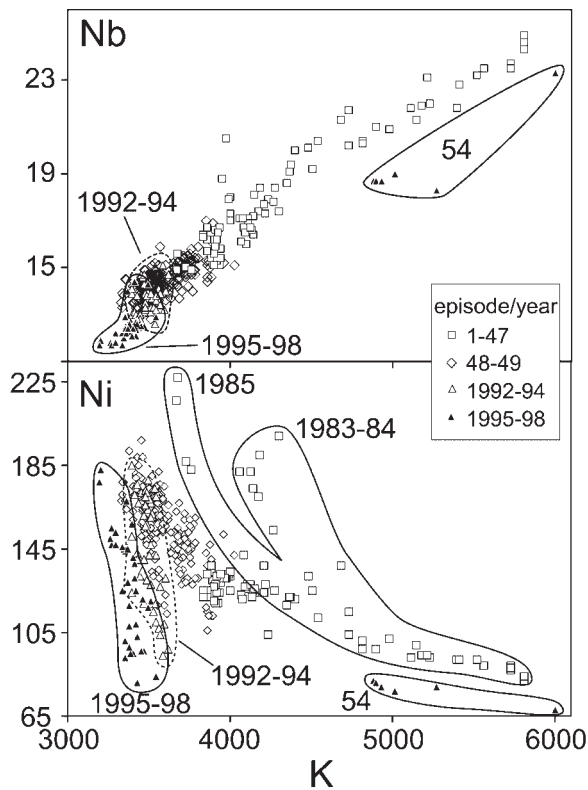
Fig. 4. Variation of Nb and Ni vs K (all in ppm) for Pu'u 'O'o lavas (fields and symbols are as in Fig. 3 except the episode 50–53 and 55 lavas have been subdivided by date of eruption, 1992–1994 and 1995–1998; data from Table 5). The shift towards lower incompatible element abundance with time (except for episode 54 lavas) and the large variation in Ni at a given K concentration relative to analytical error (about symbol size) should be noted. All values are in ppm.

anomalous cpx pressure estimates. It was assumed for this modeling that the magma underwent equilibrium crystallization, contained 0·3 wt % H_2O and 0·1 wt % CO_2, and that its redox state was one log unit below the FMQ (fayalite–magnetite–quartz) buffer (models were also run at FMQ with no significant change in the results). The model results indicate that olivine is the liquidus phase only at low pressures (<0·3 GPa). At moderate pressures (0·3–0·6 GPa), orthopyroxene is the liquidus phase, rather than cpx, and olivine is unstable. Euhedral olivine is ubiquitous in all but the most evolved Pu'u 'O'o lavas and orthopyroxene has not been observed in any of the Pu'u 'O'o lavas. Previous studies have consistently shown that cpx phenocrysts are rare in Kilauea lavas, except those with MgO contents <6·8 wt % (e.g. lavas with ∼5 wt % MgO from the 1955 eruption contain cpx; Macdonald & Eaton, 1964). Therefore, the calculated moderate pressure for cpx crystallization in Pu'u 'O'o magmas is probably an artifact of their rapid growth (as discussed above). The moderate CaO content of the Pu'u 'O'o olivines (0·25–0·32 wt %, except in the

black olivines; Table 3) is consistent with results of the MELTS calculations that olivine formed at low pressures (e.g. Ulmer, 1989). Thus, it is our conclusion that the minerals in the Pu'u 'O'o lavas record only the effects of low-pressure processes (<0·3 GPa).

If the shallow magmatic processes in the rift zone and Pu'u 'O'o reservoir can be identified and their compositional effects removed from the geochemistry of Pu'u 'O'o lavas, then the geochemical signature of mantle melting and source heterogeneity can be identified. In the following sections, we present an analysis of the crustal and mantle magmatic processes affecting Pu'u 'O'o lavas.

CRUSTAL MAGMATIC PROCESSES FOR THE PU'U 'O'O ERUPTION
Olivine fractionation and accumulation

The importance of olivine in controlling compositional variation in Hawaiian tholeiitic lavas has been recognized for many years (e.g. Powers, 1955). This observation is reaffirmed in Pu'u 'O'o lavas by the presence of only normally zoned, olivine phenocrysts and the relatively high and nearly constant whole-rock CaO/Al_2O_3 (∼0·83) in all Pu'u 'O'o lavas erupted since episode 20 in 1984 (except those from episode 54). In addition to olivine fractionation, olivine accumulation is important in these weakly to moderately olivine-phyric lavas. For example, during a 4 month period of episode 53, the lavas exhibit the largest MgO variation (7·1–10·1 wt %) since the onset of continuous effusion in 1986 but have essentially the same olivine composition (81·0 ± 0·5% Fo). The overall MgO variation for the two extreme lavas from this period (samples 11-Sep-95, which has olivine in equilibrium with a melt of its whole-rock composition, and 19-Jan-96, the most MgO-rich lava from the entire eruption) can be explained by accumulation of ∼6·9 vol. % olivine with 81% Fo. This result is consistent with the relatively large difference in olivine abundance in these two samples (5·8 ± 1·5 vol. %). Good agreement between predicted and observed olivine differences is also found for the less MgO-rich sample 14-Oct-95 (8·9 wt %) and sample 11-Sep-95 (predicted 3·9 vol. % vs observed 3·6 ± 0·8 vol. %). These results are consistent with the observation that most of the MgO-rich, episode 50–53 lavas have olivine forsterite contents too low to be in equilibrium with their host rocks (Fig. 2). Thus, the episode 50–53 melts probably accumulated olivine and were less MgO rich than the episode 48 magmas.

Crustal assimilation

Pu'u 'O'o lavas have relatively low matrix oxygen isotope ratios (4·6–5·2‰) and the oxygen isotope ratios for olivines in many of these lavas are out of equilibrium with

Table 7: *ICP-MS analyses of selected Pu'u 'O'o lavas from episodes 50 to 55*

Episode	Sample	Day	Rb	Cs	Ba	La	Ce	Pr	Nd	Sm	Eu	Gd	Tb	Dy	Ho	Er	Tm	Yb	Lu	Th	Y	Nb	Hf	U
51	12-Mar-92	3356	7.5	0.072	100	11.4	28.5	4.29	19.6	5.25	1.80	5.61	0.86	5.18	0.97	2.55	0.35	2.04	0.29	0.87	27.8	12.2	3.71	0.295
51	06-Jun-92	3442	7.7	0.078	106	12.1	29.9	4.42	20.7	5.61	1.95	5.99	0.92	5.42	1.02	2.68	0.38	2.18	0.32	0.88	28.8	12.4	3.99	0.301
51	08-Sep-92	3536	7.1	0.071	99	11.4	28.5	4.21	19.5	5.16	1.83	5.60	0.84	5.04	0.94	2.46	0.35	1.98	0.28	0.82	28.0	12.6	3.69	0.281
51	12-Nov-92	3601	7.8	0.075	104	11.9	30.3	4.48	20.4	5.57	1.92	5.83	0.91	5.40	1.04	2.73	0.39	2.16	0.31	0.85	28.4	12.4	3.89	0.297
51	29-Dec-92	3648	7.2	0.072	103	11.7	29.0	4.35	20.0	5.34	1.88	5.96	0.88	5.19	0.98	2.58	0.37	2.05	0.29	0.87	28.4	12.8	3.84	0.293
53	20-Feb-93	3701	7.6	0.069	99	11.3	28.7	4.33	19.9	5.28	1.83	5.76	0.86	5.05	0.97	2.53	0.35	2.06	0.29	0.90	27.4	12.4	3.79	0.286
53	09-May-93	3779	7.3	0.066	99	11.2	28.1	4.15	19.1	5.09	1.81	5.57	0.83	4.92	0.93	2.47	0.34	2.00	0.28	0.81	26.8	12.6	3.73	0.284
53	13-Aug-93	3875	7.9	0.072	108	11.9	30.3	4.41	20.3	5.64	1.93	5.93	0.89	5.38	1.03	2.66	0.37	2.16	0.30	0.92	28.3	13.2	4.05	0.316
53	04-Jan-94	4019	7.9	0.075	106	11.8	29.9	4.42	20.7	5.45	1.90	5.94	0.88	5.34	0.99	2.57	0.37	2.12	0.30	0.90	28.5	12.9	3.88	0.321
53	25-Apr-94	4130	8.1	0.076	109	12.3	30.8	4.63	21.4	5.73	1.97	6.21	0.91	5.58	1.04	2.77	0.37	2.21	0.30	0.92	29.3	13.3	4.05	0.320
53	25-Aug-94	4252	7.8	0.072	102	11.5	28.6	4.29	19.6	5.29	1.84	5.88	0.86	5.22	0.98	2.57	0.36	2.11	0.29	0.84	27.9	13.3	3.90	0.292
53	09-Oct-94	4297	7.5	0.071	104	11.7	29.3	4.32	20.1	5.35	1.89	5.79	0.87	5.09	0.98	2.55	0.36	2.08	0.30	0.85	27.0	13.1	3.88	0.300
53	14-Jan-95	4394	7.5	0.072	102	11.4	29.3	4.30	20.1	5.46	1.85	5.76	0.87	5.21	0.95	2.61	0.36	2.10	0.29	0.90	27.5	13.0	3.88	0.304
53	27-Apr-95	4497	7.6	0.075	98	11.1	28.0	4.20	19.0	5.19	1.87	5.58	0.88	5.03	0.95	2.49	0.35	2.12	0.29	0.89	27.8	13.0	3.75	0.288
53	15-Aug-95	4607	7.2	0.071	98	11.3	28.9	4.27	19.5	5.21	1.80	5.75	0.86	5.13	0.99	2.59	0.36	2.10	0.29	0.85	27.5	12.9	3.90	0.290
53	14-Oct-95	4667	7.4	0.068	99	11.0	27.5	4.06	18.6	5.18	1.79	5.67	0.85	5.03	0.95	2.50	0.35	2.02	0.28	0.85	27.3	12.7	3.74	0.291
53	19-Jan-96	4764	6.7	0.062	91	10.4	26.3	3.91	18.1	4.92	1.69	5.19	0.80	4.76	0.90	2.43	0.33	1.91	0.27	0.81	25.7	11.8	3.56	0.279
53	15-Mar-96	4820	7.2	0.067	97	11.0	27.7	4.17	18.9	5.15	1.78	5.71	0.85	5.19	0.98	2.56	0.36	2.12	0.29	0.83	27.2	12.6	3.88	0.290
53	07-Jun-96	4904	7.2	0.071	100	11.4	28.8	4.27	19.9	5.33	1.90	5.66	0.87	5.26	0.99	2.61	0.35	2.12	0.29	0.84	27.3	12.4	3.88	0.272
53	22-Aug-96	4980	7.6	0.072	101	11.6	29.0	4.33	19.8	5.32	1.86	5.72	0.86	5.19	0.99	2.55	0.36	2.08	0.29	0.93	29.0	12.6	3.80	0.317
53	10-Jan-97	5121	7.4	0.065	94	10.7	26.7	4.01	18.3	4.95	1.74	5.44	0.81	4.89	0.93	2.44	0.34	1.98	0.28	0.84	27.8	12.8	3.58	0.284
54	Vent F	5141	13.4	0.129	181	20.5	49.9	7.31	31.6	7.95	2.66	8.32	1.24	7.25	1.36	3.54	0.49	2.91	0.39	1.57	37.1	23.2	6.09	0.553
54	Vent B	5141	11.0	0.100	151	16.9	41.4	6.04	27.3	6.76	2.29	7.10	1.04	6.06	1.15	2.99	0.41	2.42	0.34	1.27	32.3	19.0	5.09	0.430
54	Vent E	5141	11.3	0.102	148	16.2	40.0	5.81	26.0	6.62	2.25	7.02	1.03	5.98	1.12	2.94	0.41	2.40	0.33	1.28	32.4	18.6	4.89	0.433
55	30-Jan-97	5141	7.5	0.075	100	11.6	29.3	4.38	19.9	5.46	1.91	5.81	0.88	5.24	1.01	2.62	0.37	2.17	0.30	0.89	28.2	12.5	3.84	0.302
55	21-Apr-97	5222	7.4	0.069	101	11.4	28.8	4.15	19.6	5.31	1.89	5.90	0.87	5.23	0.98	2.56	0.36	2.14	0.30	0.84	27.9	13.0	3.88	0.285
55	23-Jul-97	5315	7.2	0.068	97	10.9	27.3	4.13	19.3	5.17	1.79	5.65	0.85	4.99	0.95	2.53	0.35	2.06	0.29	0.81	28.1	12.7	3.75	0.274
55	10-Jan-98	5486	6.9	0.065	92	10.4	26.5	3.96	18.2	4.91	1.74	5.42	0.81	4.81	0.91	2.38	0.34	1.97	0.27	0.75	26.5	11.6	3.58	0.266

Day is the number of days since the start of the Pu'u 'O'o eruption (Jan. 03, 1983); all values are in ppm.
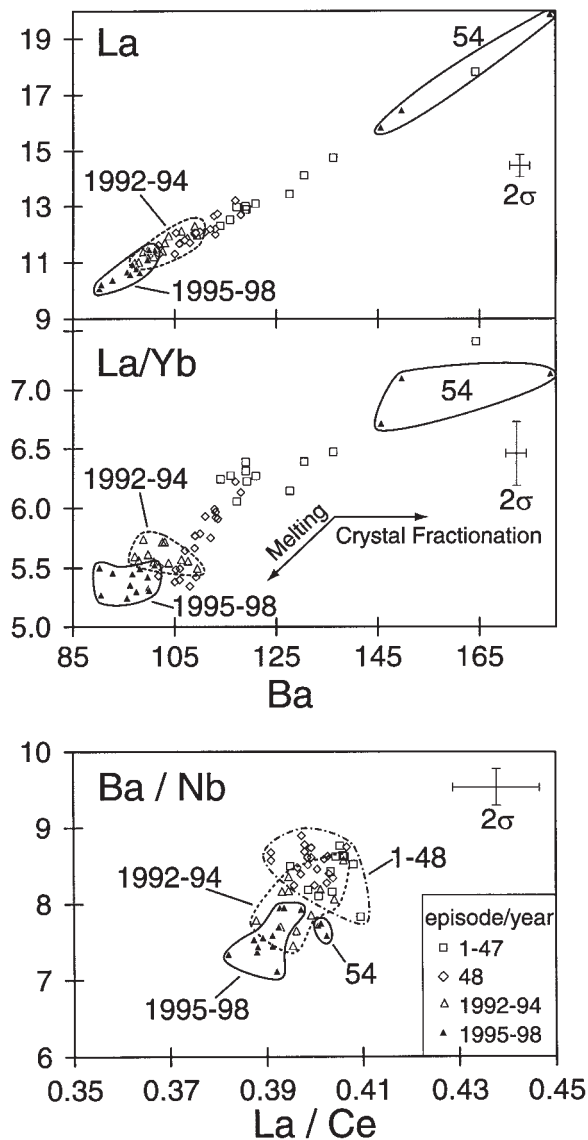
Fig. 5. Trace element variation in Pu'u 'O'o lavas based on ICP-MS data (fields and symbols are as in Fig. 4; data from Table 6). Plots of highly incompatible elements (e.g. La vs Ba) define linear trends with decreasing values with time (except for episode 54 lavas). The scatter on this plot is almost within analytical error (2σ error bars given for reference). There is an overall decrease in La/Yb ratio with time (except for episode 54 samples). The large range in Ba and La for the episode 54 rocks is probably due to extensive crystal fractionation. The plot of highly incompatible element ratios shows a tight data cluster for episode 1–48 lavas but distinctly lower ratios for some episode 50–55 lavas.

the matrix (Garcia *et al.*, 1998*a*). This disequilibrium is thought to have occurred after the growth of olivine because some of the olivines have oxygen isotope values consistent with growth from a 'normal' mantle-derived magma (~5·5‰; Garcia *et al.*, 1998*a*). The size of the oxygen isotope disequilibrium between olivine and matrix

does not correlate with major and trace element concentrations or ratios, or with the Pb, Sr or Nd isotope compositions of Pu'u 'O'o lavas. Therefore, Pu'u 'O'o magmas probably partially assimilated and exchanged oxygen with a high-temperature metamorphosed Kilauea basalt (Garcia *et al.*, 1998*a*). The presence of basaltic xenoliths with black olivines in some Pu'u 'O'o lavas may be related to this process. The amount of crustal assimilation was greatest (perhaps up to 12%) during the early period of magma mixing with rift-zone stored magmas but decreased dramatically or stopped following the shift to continuous effusion in 1986 (Garcia *et al.*, 1998*a*).

Magma mixing: episode 54 lavas

Previous studies of Kilauea's historical eruptions have focused on the products of short-lived eruptions and found that magma mixing involving a differentiated, rift zone-stored magma and the influx of a more MgO-rich magma is a common process (e.g. Wright & Fiske, 1971). The lavas from the first 2 years of the Pu'u 'O'o eruption display ample petrographic, mineral and whole-rock chemical evidence of magma mixing (Garcia *et al.*, 1992). Except for the rare high-Fo (87–89%) olivines, which may be relics from the influx of new magma, there is no evidence of magma mixing in Pu'u 'O'o lavas erupted from episodes 30 to 54 (a 12 year period).

Episode 54 marked an abrupt change in lava mineralogy and composition when evolved lavas with rare plagioclase phenocrysts (Tables 2 and 4) erupted a few kilometers up-rift from the Pu'u 'O'o cone (Fig. 1). The start of episode 54 was accompanied by rapid subsidence of Kilauea's summit and an intrusion into the rift zone (Heliker *et al.*, 1998*a*). The episode 54 lavas have distinct differences in mineralogy and whole-rock geochemistry from early 1983, evolved lavas (Figs 3–5), which were erupted from the same area. These differences indicate that they were derived from compositionally distinct magmas. The mixing event for episode 54 lavas probably occurred shortly before eruption. Otherwise, the high Fo content olivines in the hybrid lavas would have been partially or completely re-equilibrated by diffusion. No suitable mixing end members are evident among the Pu'u 'O'o lavas for the episode 54 lavas because the F vent sample does not lie on a mixing trend with the other episode 54 lavas (Fig. 3). These results suggest that Kilauea's east rift zone, a site of frequent intrusions over the last 50 years (Klein *et al.*, 1987), contains many closely spaced pockets of compositionally distinct magma that can be forced to erupt by intruding dikes as suggested by Ho & Garcia (1988).

In summary, the dominant crustal processes modifying the geochemistry of Pu'u 'O'o magmas are fractionation

Table 8: Pb, Sr and Nd isotopic data for selected Pu'u 'O'o eruption lavas

Sample	Episode	$^{206}Pb/^{204}Pb$	$^{207}Pb/^{204}Pb$	$^{208}Pb/^{204}Pb$	$^{87}Sr/^{86}Sr$	$^{143}Nd/^{144}Nd$
29-Dec-92*	51	18·397	15·460	38·016	0·703601	0·512956
25-Apr-94*	53	18·407	15·472	38·058	0·703605	0·512957
27-Apr-95	53	18·427	15·492	38·105	0·703607	0·512955
10-Jan-97	53	18·414	15·480	38·067	0·703604	0·512953
10-Jan-98	55	18·429	15·502	38·139	0·703610	0·512950

All isotopic measurements were made using the VG Sector solid source mass spectrometer at the University of Hawaii. Nd and Sr isotopic fractionation corrections are $^{148}Nd/^{144}Nd = 0·241572$ and $^{86}Sr/^{88}Sr = 0·1194$. The data are reported relative to standard values for La Jolla Nd ($^{143}Nd/^{144}Nd = 0·511844$) and NBS 981 Sr ($^{87}Sr/^{86}Sr = 0·710258$). Pb isotopic ratios are corrected for fractionation using the NBS 981 Pb standard values of Todt *et al.* (1984). The estimated uncertainties (1σ) are based on repeated measurements of the standards: $^{206}Pb/^{204}Pb$ and $^{207}Pb/^{204}Pb \pm 0·006$, $^{208}Pb/^{204}Pb \pm 0·017$; $^{87}Sr/^{86}Sr \pm 0·000012$, $^{143}Nd/^{144}Nd \pm 0·000009$. Total procedural blanks are negligible: 10–80 pg for Pb, <120 pg for Sr and <20 pg for Nd. *Data from Garcia *et al.* (1996).
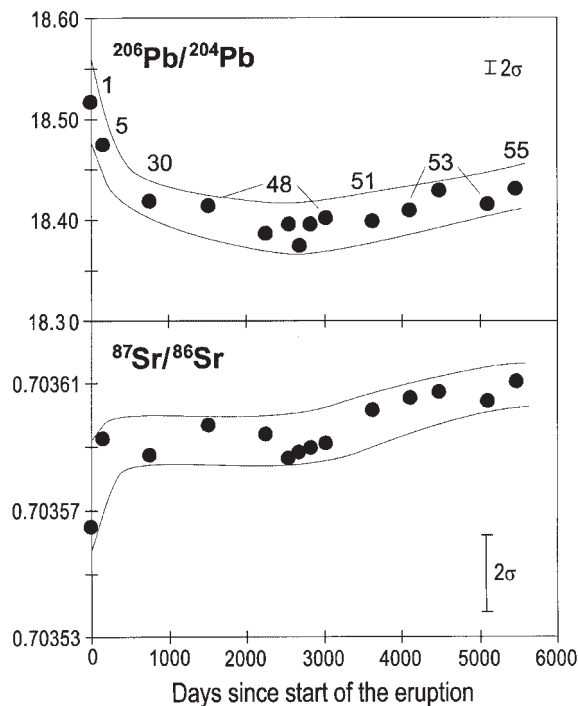
Fig. 6. Variation in $^{206}Pb/^{204}Pb$ and $^{87}Sr/^{86}Sr$ with time for the Pu'u 'O'o eruption (data from Table 7). Pb isotopes show the greatest variation compared with analytical error, with most of the variation within the first 2 years of the eruption (a period of magma mixing). The Sr isotope ratio data define a similar but less well-defined trend because of the small variation in this ratio relative to analytical error (see 2σ error bars).

Fig. 7. $^{206}Pb/^{204}Pb$ and $^{87}Sr/^{86}Sr$ ratios for recent Hawaiian tholeiitic lavas from Kilauea, Loihi and Mauna Loa volcanoes [data from Pietruszka & Garcia (1999a) for Kilauea, Garcia *et al.* (1993, 1995, 1998b) for Loihi, and Kurz *et al.* (1995) and Rhodes & Hart (1995) for Mauna Loa]. The wide scatter in Pb and Sr isotopes for recent lavas from these closely space volcanoes (triangle, Mauna Loa 1975 eruption; square, Loihi, 1996) requires at least three source components in the Hawaiian plume. The Pu'u 'O'o lavas deviate with the well-defined negative trend for Mauna Loa and other Kilauea lavas; instead, they trend towards and overlap with the Loihi field.

and accumulation of olivine. Crustal assimilation and magma mixing have been important only during the early part of the eruption and during episode 54.

MANTLE-RELATED TEMPORAL GEOCHEMICAL VARIATIONS

The whole-rock compositions of the non-hybrid Pu'u 'O'o lavas from 1985 to 1998 were normalized to the same 'parental' MgO content to allow an evaluation to be made of the mantle-related geochemical variations for this eruption. A value of 10 wt % MgO was selected for normalization because it corresponds to the most MgO-rich Pu'u 'O'o lava composition. Furthermore, the higher forsteritic olivines (85%) from this eruption are in equilibrium with a melt of this MgO content, assuming

90% of the total iron is Fe^{2+}. Because olivine is the only phenocryst in these lavas, the normalization was performed using a mixture of 98·5% equilibrium olivine and 1·5% Cr-spinel, a typical proportion of these minerals in Kilauea lavas (Wright, 1971), added in small increments (0·02%) to the liquid.

The results of this normalization procedure indicate that highly incompatible elements (e.g. K) and CaO decrease systematically with time (Fig. 8), Al_2O_3, Y and Yb remain essentially constant, whereas Fe_2O_3 and SiO_2 slightly increase. These results extend the trends that were identified for the 1985–1992 period of the Pu'u 'O'o eruption (Garcia *et al.*, 1996) and clearly demonstrate a long-term systematic compositional variation for the eruption. A systematic decrease in the abundance of incompatible elements was also noted for the 1969–1974 Mauna Ulu eruption of Kilauea (Hofmann *et al.*, 1984).

MANTLE MELTING MODELS FOR TWO PROLONGED KILAUEA ERUPTIONS

The magmas for the Pu'u 'O'o and Mauna Ulu rift zone eruptions of Kilauea are thought to have partially bypassed the volcano's summit magma storage reservoir (Ryan *et al.*, 1981; Garcia *et al.*, 1996). Thus, these eruptions potentially offer a more direct view of the processes that generate tholeiitic basalts in the Hawaiian mantle plume compared with Kilauea's historical summit lavas, which are thought to have been stored in the summit reservoir for ∼30–120 years (Pietruszka & Garcia, 1999*b*). Unlike these summit lavas (Pietruszka & Garcia, 1999*a*), lavas from these two rift zone eruptions display a rapid decrease in the abundance of highly incompatible elements (e.g. K, Nb) and in ratios of highly to moderately incompatible trace elements (i.e. Ce/Yb) with little or no change in Pb, Sr and Nd isotope ratios (Hofmann *et al.*, 1984; Figs 6 and 8). There are, however, important geochemical differences between these two eruptions. The CaO contents of the Pu'u 'O'o eruption lavas decreased over time (Fig. 8), whereas no change in the CaO abundance of the Mauna Ulu lavas erupted from 1969 to 1971 was observed (Hofmann *et al.*, 1984). Furthermore, ratios of highly incompatible trace elements (e.g. Ba/Ce) also decreased slightly over time for the Pu'u 'O'o lavas, whereas these ratios are constant in the Mauna Ulu lavas (Hofmann *et al.*, 1984; Fig. 8). The incompatible trace element ratio changes for both eruptions are consistent with the relative incompatibility of these elements during mantle melting (e.g. Hauri *et al.*, 1994). This suggests that partial melting processes, rather than source heterogeneity, are the dominant controls on
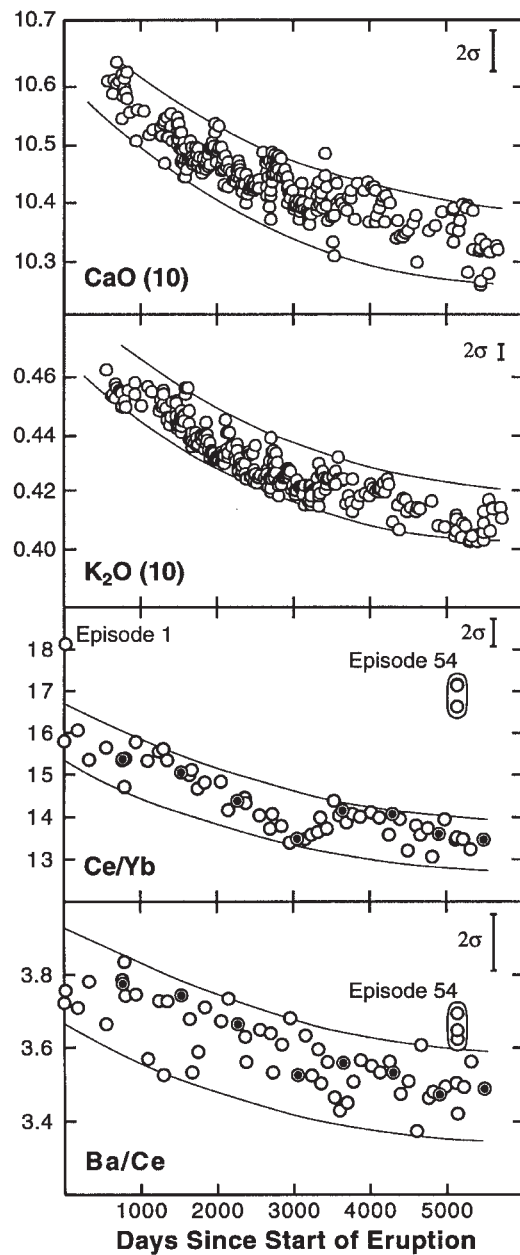
Fig. 8. Temporal variation of CaO and K_2O contents (normalized to 10 wt % MgO, the most MgO-rich composition erupted from Pu'u 'O'o; see text for description of the normalization procedure), Ce/Yb and Ba/Ce ratios for Pu'u 'O'o lavas [data from Tables 5 and 6 and Garcia *et al.* (1992, 1996)]. The overall decrease in these variables during the course of the eruption should be noted. These changes require a depletion in the source for Pu'u 'O'o lavas with time. ● (on the ratio plots), samples used for the modeling shown in Table 8, which was constrained to produce the observed ratios for Ce/Yb and Ba/Ce. The 2σ errors are given in the upper right corner of each plot.

the compositional variation for these lavas. Below, we evaluate two models that have been proposed to explain the large compositional variation in prolonged Kilauea

eruptions with little or no change in Pb, Sr and Nd isotopes: batch melting of a homogeneous source (Hofmann *et al.*, 1984) and progressive source depletion through mantle melting (Garcia *et al.*, 1996).

Both melting models require an estimate of the degree of partial melting for the earliest Pu'u 'O'o lavas. We chose an initial melt fraction of 10% for Pu'u 'O'o lavas based on our previous results of modeling Kilauea historical lavas (Pietruszka & Garcia, 1999*a*). This estimate is derived from the systematic temporal variations in Pb, Sr and Nd isotope and incompatible trace element ratios at this volcano over the last 200 years, which are thought to result from the short-term changes in the composition of the mantle source and the degree of partial melting. In the context of this model, Pu'u 'O'o lavas formed at relatively high melt fractions compared with other historical Kilauea lavas, on the basis of their low ratios of highly over moderately incompatible trace elements (e.g. Ce/Yb). The source mineralogy and the melting mode for the melting model are essentially the same as used by Hofmann *et al.* (1984) for the Mauna Ulu eruption. We found that the modeling results were rather insensitive to the melting mode, which was also pointed out by Hofmann *et al.* (1984).

Batch melting of a homogeneous source

The temporal decrease in ratios of highly over moderately incompatible trace elements for Mauna Ulu lavas can be explained by a 20% relative increase in the degree of batch partial melting during the eruption (Hofmann *et al.*, 1984). This model is consistent with the relatively constant ratios of Sr and Nd isotopes and of highly incompatible trace elements (e.g. Ba/Ce) in lavas from this eruption. A similar model for Pu'u 'O'o lavas (see Table 9 for model parameters) also requires an ∼20% relative increase in the degree of partial melting to explain the variation in ratios of highly over moderately incompatible trace element (Ce/Yb; Fig. 8). However, a simple increase in the degree of partial melting cannot account for the slight temporal decrease of highly incompatible trace element ratios observed for Pu'u 'O'o lavas (e.g. Ba/Ce; Fig. 8) as a result of the relatively high melt fraction expected for Kilauea tholeiites (5–10%; Pietruszka & Garcia, 1999*a*). Furthermore, this batch melting model is inconsistent with experimental results (Kushiro, 1996) for partial melting of a fertile garnet lherzolite source at 3 GPa (the mantle source conditions that are thought to be needed for generation of Kilauea magmas; Hofmann *et al.*, 1984), which show that CaO should increase with increasing degrees of partial melting up to ∼20% (when cpx disappears). This expected increase in CaO content with increasing degree of partial melting was not observed for the Mauna Ulu eruption

(Hofmann *et al.*, 1984) and a decrease with time was observed for the Pu'u 'O'o eruption (Fig. 8).

Progressive melting and source depletion

Alternately, the temporal decrease in the incompatible trace element ratios (e.g. Ce/Yb and Ba/Ce) of Pu'u 'O'o lavas may result from an increase in the proportion of melt derived from a depleted source component. The relatively constant Pb, Sr and Nd isotope ratios of Pu'u 'O'o lavas suggest that this depletion is a recent consequence of melting within the Hawaiian plume. In this context, Garcia *et al.* (1996) proposed that the geochemical variations of Pu'u 'O'o lavas were caused by an eruption-related modification of the Kilauea's mantle source through progressive mantle melting and depletion. Their model assumed that the later Pu'u 'O'o lavas formed by a simple remelting of the same source that produced the early lavas (e.g. at a constant melt fraction of 10% throughout the eruption). In testing this model, however, we discovered that it fails to explain the overall chemistry of Pu'u 'O'o lavas because the magmas generated from a remelted source would have incompatible trace element abundances and ratios much lower than observed.

To overcome this problem, we considered a more complex progressive melting model using two source components (an 'initial' and a 'depleted') with the same isotopic composition. The 'depleted' source component is assumed to have experienced a relatively small amount of prior melt removal (compared with the total melt fraction). The 'depleted' source was mixed with the 'initial' source, and this mixed source was partially melted to form the subsequent Pu'u 'O'o lavas. To determine the possible extent of previous melting for the 'depleted' source component, we evaluated a range of values from 0·1 to 10% (i.e. slightly to strongly depleted sources, respectively). Good residuals are obtained for incompatible element abundances and ratios using this model only if this parameter is <10%. If the amount of previous melting is ∼3%, the total degree of partial melting during the eruption remains nearly constant at ∼10 ± 1% (Table 9). For smaller or larger amounts of recent melt removal, the model predicts that the degree of partial melting during the Pu'u 'O'o eruption increases or decreases over time, respectively. The maximum amount of recent melt removal permitted by the model is ∼7% because, at higher values, the total melt fraction for the late Pu'u 'O'o lavas would be <5%, which is outside the range expected for Hawaiian shield lavas (5–20%; Watson, 1993). In all cases, the model results suggest that the relative amount of the 'depleted' source component increased progressively during the eruption, although magnitude depends on the amount of recent melt removal to form the 'depleted' source. For 3%

Table 9: Representative results of the mixed source progressive melting model for Pu'u 'O'o lavas

	2σ error (%)	Sources Initial	Sources Depleted	Model results KE30-362 8-Feb-85	16-Mar-87 (% Diff)	26-Mar-89 (% Diff)	12-May-91 (% Diff)	29-Dec-92 (% Diff)	09-Oct-94 (% Diff)	07-Jun-96 (% Diff)	10-Jan-98 (% Diff)
Rb	(6.6)	0.70	0.0017	8.3	8.2 (1.8)	8.0 (2.3)	7.4 (0.4)	7.5 (4.6)	7.5 (0.1)	7.2 (0.1)	6.7 (−3.4)
Ba	(2.2)	9.63	0.0231	114	114 (0.3)	111 (0.7)	103 (1.1)	104 (1.2)	104 (0.2)	99 (−0.6)	92 (0.1)
Th	(4.0)	0.077	0.0046	0.90	0.90 (−4.0)	0.88 (−1.1)	0.82 (−8.2)	0.83 (−3.9)	0.83 (−2.0)	0.80 (−4.4)	0.74 (−0.7)
U	(3.4)	0.0279	0.00263	0.322	0.321 (−0.3)	0.316 (2.1)	0.297 (−2.4)	0.300 (2.2)	0.299 (−0.2)	0.289 (6.0)	0.268 (0.8)
Nb	(2.4)	1.17	0.211	13.2	13.2 (3.9)	13.0 (1.9)	12.4 (0.6)	12.5 (−2.4)	12.5 (−4.8)	12.1 (−2.9)	11.2 (−3.9)
La	(3.4)	1.10	0.233	12.3	12.3 (2.2)	12.2 (0.5)	11.7 (0.2)	11.7 (0.2)	11.7 (0.0)	11.4 (0.0)	10.6 (1.2)
Ce	(3.6)	2.79	0.803	30.3	30.4 (0.3)	30.3 (0.7)	29.2 (1.1)	29.3 (1.2)	29.4 (0.2)	28.6 (−0.6)	26.5 (0.1)
Pr	(3.4)	0.434	0.189	4.36	4.39 (0.0)	4.43 (−1.0)	4.35 (−0.6)	4.34 (−0.3)	4.36 (0.9)	4.29 (0.3)	3.96 (0.0)
Nd	(2.8)	2.13	1.15	19.8	20.0 (−2.0)	20.3 (−0.9)	20.2 (−0.3)	20.0 (0.0)	20.2 (0.4)	19.9 (0.1)	18.4 (1.3)
Sm	(2.2)	0.662	0.460	5.17	5.25 (−1.0)	5.39 (−2.4)	5.44 (−1.0)	5.35 (0.1)	5.39 (0.9)	5.37 (0.8)	4.97 (1.2)
Eu	(3.8)	0.248	0.183	1.80	1.83 (−1.8)	1.88 (−1.4)	1.91 (2.7)	1.87 (−0.4)	1.89 (−0.4)	1.88 (−1.1)	1.74 (0.0)
Gd	(2.8)	0.863	0.681	5.55	5.65 (0.4)	5.84 (0.9)	5.94 (2.6)	5.79 (−2.8)	5.84 (1.0)	5.85 (3.3)	5.43 (0.1)
Dy	(3.2)	1.00	0.868	4.94	5.04 (−0.1)	5.24 (−0.8)	5.35 (1.1)	5.18 (−0.1)	5.23 (2.7)	5.25 (−0.2)	4.88 (1.6)
Er	(4.0)	0.658	0.605	2.42	2.48 (−0.7)	2.58 (−2.5)	2.65 (0.7)	2.54 (−1.4)	2.57 (0.7)	2.58 (−0.9)	2.41 (1.2)
Yb	(2.6)	0.687	0.651	1.97	2.02 (0.4)	2.11 (0.7)	2.16 (1.1)	2.07 (1.2)	2.09 (0.2)	2.11 (−0.6)	1.97 (0.1)
ΣR²	(186)				(49.0)	(33.6)	(94.2)	(61.2)	(37.5)	(79.0)	(36.4)
Ce/Yb		4.07	1.23	15.4	15.1	14.4	13.5	14.2	14.1	13.6	13.5
Ba/Ce		3.45	0.0288	3.77	3.74	3.66	3.53	3.56	3.53	3.47	3.49
% Total melt				10.0	10.0	10.0	9.8	9.3	9.1	9.2	9.5
% Depleted source				0.0	2.7	9.4	20.2	19.6	21.8	25.3	23.5

Sample KE30-362 represents the earliest Pu'u 'O'o lava that avoided magma mixing in the rift zone (Garcia *et al.*, 1996) and is thought to best represent the initial mantle-derived magma composition for this eruption. The trace element abundances of this sample were adjusted to 16 wt % MgO using the normalization procedure described in the text to create a potential parental magma composition. The 'initial' source composition was calculated from this parental magma assuming that it was produced by 10% non-modal batch partial melting (Shaw, 1970) of a source containing olivine (60%), clinopyroxene (15%), orthopyroxene (15%) and garnet (10%), which enter the melt in 3:4:2:1 proportions. The mineralogy (61% olivine, 14% clinopyroxene, 15% orthopyroxene, and 10% garnet) and trace element composition of the 'depleted' source was calculated from this 'initial' source assuming that 3% melt had been removed. These two source components were mixed (only the % of the depleted component is reported) and partially melted to a degree (% total melt) necessary to reproduce the observed Ce/Yb and Ba/Ce ratios of the lavas. These ratios were selected because they were determined with relatively high precision and are sensitive to changes in the degree of partial melting and source composition, respectively. Finally, the calculated primary magma compositions were evolved by olivine control to match the observed trace element concentrations of the lavas. The mineral–liquid partition coefficients used for the calculations are from Shimizu & Kushiro (1975), Hauri *et al.* (1994), Johnson (1998) and Salters & Longhi (1999) for garnet and clinopyroxene. The *D* values for olivine and orthopyroxene are assumed to be zero. For each lava, the model results for the incompatible trace element concentrations (in ppm), and residuals (% Diff: 100 × [(calculated/observed) − 1]) are shown. The ΣR² value for each sample is the sum of the squared % residuals for all elements. The 2σ error for each trace element is based on replicate analyses of the rock standard, Kil1919, which was run as an unknown over the course of this study (see Pietruszka & Garcia, 1999a).

recent melt removal, which gave the lowest residuals, the amount of the 'depleted' source increases from 0 to ∼25% (Table 9). Although the assumptions used in this modeling are based on previous studies, they may seem somewhat arbitrary. None the less, the modeling results demonstrate that the progressive melting model provides a better explanation for the geochemical variation of the Pu'u 'O'o lavas than other models we considered.

We favor ∼3% recent melt removal to form the 'depleted' source component (Table 9) because (1) the overall lava output rate has not changed during the Pu'u 'O'o eruption and (2) a small value for this factor is required to account for the subtle temporal decrease in the Th/U, Ba/Th, and Ba/U ratios of Pu'u 'O'o lavas (as determined by high-precision isotope dilution methods; A. Pietruszka, unpublished data, 1999). Physically, this removed melt could have been incorporated into the early eruptive products of Pu'u 'O'o, a previous Kilauea eruption, or, possibly, an eruption from the adjacent younger volcano, Loihi. If the amount of melt removal was ∼3%, then it is unlikely to be related to a Kilauea eruption during its shield stage (last 400 ky; Quane et al., 2000) because the range in melt fractions for Hawaiian tholeiitic basalts is expected to be higher (5–20%; Watson, 1993). Kilauea's melting region may have progressively encroached upon a source that was melted to form Loihi's alkalic and transitional lavas, which are thought to have formed by lower degrees of melting than tholeiitic lavas (e.g. Watson, 1993). Three additional lines of evidence favor a Loihi source: (1) Pu'u 'O'o lavas are isotopically similar to some Loihi lavas (Fig. 7); (2) U-series model results suggest that Pu'u 'O'o is tapping a relatively large mantle source region, which may overlap with that of Loihi (Pietruszka et al., 2000); (3) the mantle conduit for Kilauea dips south towards Loihi Volcano (Tilling & Dvorak, 1993).

CONCLUSIONS

The Pu'u 'O'o eruption is noteworthy in the historical eruption record of Kilauea for its long duration, large volume, and substantial lava geochemical variation. These features, and the simple mineralogy and pristine nature of the Pu'u 'O'o lavas, have allowed us to examine both crustal magmatic and mantle melting processes. The dominant crustal processes influencing compositional variations in Pu'u 'O'o lavas are olivine fractionation and accumulation. Shallow magma mixing and crustal assimilation were important only during the early part of the eruption and episode 54. The short-term (days to weeks) geochemical variations caused by olivine fractionation and accumulation are superimposed on longer-term variations that are probably related to partial melting processes in the mantle plume. The small but systematic decrease in ratios of highly incompatible elements cannot be explained by batch melting of a homogeneous source, as was invoked for the Mauna Ulu eruption, nor can a simple progressive melting model explain them. Instead, Pu'u 'O'o magmas appear to have been produced by melting a mixed source with both components having the same isotopic composition. The depleted source component was probably previously melted by ∼3% relative to the initial source component. The percentage of the depleted component in Pu'u 'O'o lavas progressively increasing during the eruption from 0 to ∼25%. The depleted source must have formed recently to have avoided a change in its Pb, Sr and Nd isotope composition but is probably not related to a Kilauea shield stage eruption because its extent of melting was too low. Given the isotopic similarity of lavas from Pu'u 'O'o to many from the adjacent, younger volcano, Loihi, the melting region for the two volcanoes may partially overlap.

Prolonged eruptions such as Pu'u 'O'o offer an opportunity for a better understanding of crustal and mantle magmatic processes within active volcanoes. It will be interesting to see if the lessons learned from this eruption are applicable to eruptions at other oceanic island volcanoes.

REFERENCES

Fodor, R. V., Keil, K. & Bunch, T. E. (1975). Contributions to the mineral chemistry of Hawaiian rocks. IV. Pyroxenes in rocks from Haleakala and West Maui volcanoes. *Contributions to Mineralogy and Petrology* **50**, 173–195.

Garcia, M. O. & Wolfe, E. W. (1988). Petrology of the erupted lava. *US Geological Survey Professional Paper* **1463**, 127–143.

Garcia, M. O., Ho, R. A., Rhodes, J. M. & Wolfe, E. W. (1989). Petrologic constraints on rift zone processes: results from episode 1 of the Pu'u 'O'o eruption of Kilauea volcano, Hawaii. *Bulletin of Volcanology* **52**, 81–96.

Garcia, M. O., Rhodes, J. M., Ho, R. A., Ulrich, G. & Wolfe, E. W. (1992). Petrology of lavas from episodes 2–47 of the Pu'u 'O'o eruption of Kilauea Volcano, Hawaii: evaluation of magmatic processes. *Bulletin of Volcanology* **55**, 1–16.

Garcia, M. O., Jorgenson, B., Mahoney, J., Ito, E. & Irving, T. (1993). Temporal geochemical evolution of the Loihi summit lavas: results from ALVIN submersible dives. *Journal of Geophysical Research* **98**, 537–550.

Garcia, M. O., Foss, D., West, H. & Mahoney, J. (1995). Geochemical and isotopic evolution of Loihi Volcano, Hawaii. *Journal of Petrology* **36**, 1647–1674.

Garcia, M. O., Rhodes, J. M., Trusdell, F. A. & Pietruszka, A. P. (1996). Petrology of lavas from the Pu'u 'O'o eruption of Kilauea Volcano: III. The Kupaianaha episode (1986–1992). *Bulletin of Volcanology* **58**, 359–379.

Garcia, M. O., Ito, E., Eiler, J. & Pietruszka, A. P. (1998a). Crystal contamination of Kilauea Volcano magmas revealed by oxygen isotope analysis of glass and olivine from the Pu'u 'O'o eruption lavas. *Journal of Petrology* **39**, 803–817.

Garcia, M. O., Rubin, K. H., Norman, M. D., Rhodes, J. M., Graham, D. W., Muenow, D. & Spencer, K. (1998b). Petrology and geochronology of basalt breccia from the 1996 earthquake swarm of Loihi Seamount, Hawaii: magmatic history of its 1996 eruption. *Bulletin of Volcanology* **59**, 577–592.

Ghiorso, M. S. & Sack, R. O. (1995). Chemical mass transfer in magmatic systems IV. A revised and internally consistent thermodynamic model for the interpolation and extrapolation of liquid–solid equilibria in magmatic systems at elevated temperatures and pressures. *Contributions to Mineralogy and Petrology* **119**, 197–212.

Gillard, D., Rubin, A. & Okubo, P. (1996). Highly concentrated seismicity caused by deformation of Kilauea's deep magma system. *Nature* **384**, 343–346.

Harris, A. J. L., Keszthelyi, L., Flynn, L. P., Mouginis-Mark, P. J., Thornber, C., Kauahikaua, J., Sherrod, D., Trusdell, F., Sawyer, M. W. & Flament, P. (1997). Chronology of the episode 54 eruption at Kilauea Volcano, Hawaii, from GOES-9 satellite data. *Geophysical Research Letters* **24**, 3281–3284.

Hauri, E. H., Wagner, T. P. & Grove, T. L. (1994). Experimental and natural partitioning of Th, U, Pb and other trace elements between garnet, clinopyroxene and basaltic melts. *Chemical Geology* **117**, 149–166.

Heliker, C. C., Kauahikaua, J. P., Sherrod, D. R. & Thornber, C. R. (1998a). The rise and fall of the Pu'u 'O'o cone, Kilauea Volcano, 1983–1998. *EOS Transactions, American Geophysical Union* **79**, F956.

Heliker, C., Mangan, M. T., Mattox, T. N., Kauahikaua, J. P. & Helz, R. T. (1998b). The character of long-term eruptions: inferences from episodes 50–53 of the Pu'u 'O'o–Kupaianaha eruption of Kilauea Volcano. *Bulletin of Volcanology* **59**, 381–393.

Helz, R. T. & Thornber, C. R. (1987). Geothermometry of Kilauea Iki lava lake, Hawaii. *Bulletin of Volcanology* **49**, 651–668.

Ho, R. A. & Garcia, M. O. (1988). Origin of differentiated lavas at Kilauea Volcano, Hawaii: implications from the 1955 eruption. *Bulletin of Volcanology* **50**, 35–46.

Hoffmann, J. P., Ulrich, G. E. & Garcia, M. O. (1990). Horizontal ground deformation patterns and magma storage during the Pu'u 'O'o eruption of Kilauea volcano, Hawaii: episodes 22–42. *Bulletin of Volcanology* **52**, 522–531.

Hofmann, A. W., Feigenson, M. D. & Raczek, I. (1984). Case studies on the origin of basalt, III. Petrogenesis of the Mauna Ulu eruption, Kilauea 1969–1971. *Contributions to Mineralogy and Petrology* **88**, 24–35.

Holcomb, R. (1987). Eruptive history and long-term behavior of Kilauea Volcano. *US Geological Survey Professional Paper* **1350**, 261–350.

Johnson, K. T. M. (1998). Experimental determination of partition coefficients for rare earth and high-field strength elements between clinopyroxene, garnet, and basaltic melt at high pressures. *Contributions to Mineralogy and Petrology* **133**, 60–68.

Kauahikaua, J., Mangan, M., Heliker, C. & Mattox, T. (1996). A quantitative look at the demise of a basaltic vent: the death of Kupaianaha, Kilauea Volcano, Hawaii. *Bulletin of Volcanology* **57**, 641–648.

King, A., Waggoner, G. & Garcia, M. O. (1993). Geochemistry and petrology of basalts from ODP Leg 136. *Ocean Drilling Program Scientific Results, 136*. College Station, TX: Ocean Drilling Program, pp. 107–118.

Klein, F. W., Koyanagi, R. Y., Nakata, J. S. & Tanigawa, W. R. (1987). The seismicity of Kilauea's magma system. *US Geological Survey Professional Paper* **1350**, 1019–1185.

Koyanagi, R. Y., Tanigawa, W. R. & Nakata, J. S. (1988). Seismicity associated with the eruption. *US Geological Survey Professional Paper* **1463**, 183–235.

Kurz, M. D., Kenna, T. C., Kammer, D., Rhodes, J. M. & Garcia, M. O. (1995). Isotopic evolution of Mauna Loa volcano: a view from the submarine southwest rift. *American Geophysical Union Monograph* **92**, 289–306.

Kushiro, I. (1996). Partial melting of a fertile mantle peridotite at high pressures: an experimental study using aggregates of diamond. *American Geophysical Union Monograph* **95**, 109–122.

Lofgren, G. (1980). Experimental studies on the dynamic crystallization of silicate melts. In: Hargraves, R. B. (ed.) *Physics of Magmatic Processes*. Princeton, NJ: Princeton University Press, pp. 487–551.

Macdonald, G. A. (1944). Unusual features in ejected blocks at Kilauea Volcano. *American Journal of Science* **242**, 322–326.

Macdonald, G. A. & Eaton, J. P. (1964). Hawaiian volcanoes during 1955. *US Geological Survey Bulletin* **1171**, 1–85.

Macdonald, G. A., Abbott, A. T. & Peterson, F. L. (1983). *Volcanoes in the Sea*. Honolulu, HI: University of Hawaii Press, pp. 89–81.

Mangan, M. T., Heliker, C. C., Mattox, T. N., Kauahikaua, J. P. & Helz, R. T. (1995). Episode 49 of the Pu'u 'O'o–Kupaianaha eruption of Kilauea volcano—breakdown of a steady-state eruptive era. *Bulletin of Volcanology* **57**, 127–135.

Moore, J. G. & Ault, W. U. (1965). Historic littoral cones in Hawaii. *Pacific Science* **19**, 3–11.

Pietruszka, A. P. & Garcia, M. O. (1999a). A rapid fluctuation in the mantle source and melting history of Kilauea Volcano inferred from the geochemistry of its historical summit lavas (1790–1982). *Journal of Petrology* **40**, 1321–1342.

Pietruszka, A. P. & Garcia, M. O. (1999b). The size and shape of Kilauea Volcano's summit magma storage reservoir: a geochemical probe. *Earth and Planetary Science Letters* **167**, 311–320.

Pietruszka, A. P., Rubin, K. H. & Garcia, M. O. (2000). ^{226}Ra–^{230}Th–^{238}U disequilibria of historical Kilauea lavas (1790–1982) and the dynamics of mantle melting within the Hawaiian plume. *Earth and Planetary Science Letters* (submitted).

Powers, H. (1955). Composition and origin of basaltic magma of the Hawaiian Islands. *Geochimica et Cosmochimica Acta* **7**, 77–107.

Putirka, K. (1997). Magma transport at Hawaii: inferences based on igneous thermobarometry. *Geology* **27**, 69–72.

Putirka, K., Johnson, M., Kinzler, R., Longhi, J. & Walker, D. (1996). Thermobarometry of mafic igneous rocks based on clinopyroxene–

liquid equilibria, 0–30 kbar. *Contributions to Mineralogy and Petrology* **123**, 92–108.

Quane, S. L., Garcia, M. O., Guillou, H. & Hulsebosch, T. P. (2000). Magmatic history of the east rift zone of Kilauea Volcano, Hawaii based on drill core from SOH 1. *Journal of Volcanology and Geothermal Research* (in press).

Rhodes, J. M. (1996). The geochemical stratigraphy of lava flows sampled by the Hawaii scientific drilling project. *Journal of Geophysical Research* **101**, 11729–11780.

Rhodes, J. M. & Hart, S. (1995). Episodic trace element and isotopic variations in historical Mauna Loa lavas: implications for magma and plume dynamics. *American Geophysical Union Monograph* **92**, 263–288.

Roeder, P. L. & Emslie, R. F. (1970). Olivine–liquid equilibrium. *Contributions to Mineralogy and Petrology* **29**, 275–289.

Ryan, M. P., Koyanagi, R. Y. & Fiske, R. S. (1981). Modeling the three-dimensional structure of macroscopic magma transport systems. *Journal of Geophysical Research* **86**, 7111–7129.

Salters, V. J. M. & Longhi, J. (1999). Trace element partitioning during the initial stages of melting beneath mid-ocean ridges. *Earth and Planetary Science Letters* **166**, 15–30.

Shaw, D. M. (1970). Trace element fractionation during anatexis. *Geochimica et Cosmochimica Acta* **34**, 237–243.

Shimizu, N. & Kushiro, I. (1975). The partitioning of rare earth elements between garnet and liquid at high pressures: preliminary experiments. *Geophysical Research Letters* **2**, 413–416.

Staudigel, H., Zindler, A., Hart, S. R., Leslie, T., Chen, C.-Y. & Clague, D. A., (1984). The isotope systematics of a juvenile intraplate volcano: Pb, Nd, and Sr isotope ratios of basalts from Loihi seamount, Hawaii. *Earth and Planetary Science Letters* **69**, 13–29.

Tilling, R. I. & Dvorak, J. J. (1993). Anatomy of a basaltic volcano. *Nature* **363**, 125–133.

Todt, W., Cliff, R. A., Hanser, A. & Hofmann, A. W. (1984). ^{202}Pb and ^{205}Pb double spike for lead isotopic analyses. *Terra Cognita* **4**, 209.

Ulmer, P. (1989). The dependence of the Fe^{2+}–Mg cation-partitioning between olivine and basaltic liquid on pressure, temperature and composition. *Contributions to Mineralogy and Petrology* **101**, 261–273.

Ulrich, G. E., Wolfe, E. W., Heliker, C. C. & Neal, C. A. (1987). Pu'u 'O'o IV: evolution of a plumbing system. *Hawaii Symposium 1987 Abstracts Volume*, p. 259.

Watson, S. (1993). Rare earth element inversion and percolation models for Hawaii. *Journal of Petrology* **34**, 763–783.

West, H. B., Gerlach, D. C., Leeman, W. P. & Garcia, M. O. (1987). Isotopic constraints on the origin of Hawaiian lavas from the Maui Volcanic complex, Hawaii. *Nature* **330**, 216–220.

Wolfe, E. W., Garcia, M. O., Jackson, D. B., Koyanagi, R. Y., Neal, C. A. & Okamura, A. T. (1987). The Pu'u 'O'o eruption of Kilauea volcano, episodes 1 through 20, January 3, 1983, to June 8, 1984. *US Geological Survey Professional Paper* **1350**, 471–508.

Wolfe, E. W., Neal, C. A., Banks, N. G. & Duggan, T. J. (1988). Geologic observations and chronology of eruptive events. *US Geological Survey Professional Paper* **1463**, 1–97.

Wright, T. L. (1971). Chemistry of Kilauea and Mauna Loa lavas in space and time. *US Geological Survey Professional Paper* **735**, 1–45.

Wright, T. L. & Fiske, R. S. (1971). Origin of the differentiated and hybrid lavas of Kilauea Volcano, Hawaii. *Journal of Petrology* **12**, 1–65.